

Notes on Wave Propagation in Anisotropic Elastic Solids

Michael Conry
michael.conry@softhome.net

Tue Jun 18 16:20:07 IST 2002

Abstract

The aim of this document is to summarise the information on elastic material properties, and wave propagation which I have found in my recent reading. The books read are listed at the end of this document, and cited throughout. First, the basic constitutive equations governing elastic solids are presented. Once the concept of elastic properties has been established, our attention turns to the various symmetry classes which exist. These symmetries simplify the material properties. I have written more on symmetry than I had expected to, as the area turned out to be surprisingly interesting. Following on from the exposition of the material properties of various symmetry classes, we look at solving the dynamic elastic equations for specific materials. Slowness curves are introduced and calculated for particular cases.

It is important to note that this document is still a work in progress. If anyone actually *does* read it, and has suggestions/corrections, I would be very glad to hear from them at michael.conry@softhome.net

Contents

1	Basic Equations	3
2	Reduced Notation	4
3	Material Symmetry	5
3.1	Triclinic Symmetry	7
3.2	Monoclinic Symmetry	7
3.3	Orthotropic Symmetry	8

3.4	Tetragonal Symmetry	9
3.5	Trigonal Symmetry	12
3.6	Transversely Isotropic Symmetry	14
3.7	Cubic Symmetry	16
3.8	Isotropic Symmetry	16
4	Bulk Waves	17
4.1	Bulk Waves Background	17
4.2	Computation of Slowness and Skew Curves Background	18
4.3	Examples of Slowness and Skew Curves	20
4.3.1	Aluminium	20
4.3.2	InAs	20
4.3.3	Graphite-Epoxy (65%-35%)	23
4.3.4	Quartz	26
4.3.5	Cadmium Sulfide	28

List of Figures

1	Triclinic Symmetry Point Groups	7
2	Monoclinic Symmetry Point Groups	8
3	Orthotropic Symmetry Point Groups	9
4	Tetragonal Symmetry Point Groups	10
5	Trigonal Symmetry Point Groups	13
6	Hexagonal Symmetry Point Groups	15
7	Slowness Curve for Isotropic Aluminium	21
8	Slowness Curve for InAs, $\phi = 0$	22
9	Skew Curve for InAs, $\phi = 0$	23
10	Slowness Curve for InAs, $\phi = 45$	24
11	Skew Curve for InAs, $\phi = 45$	25
12	Slowness Curve for InAs, $\phi = 30$	26
13	Skew Curve for InAs, $\phi = 30$	27
14	Slowness Curve for Graphite Epoxy, $\phi = 0$	28
15	Skew Curve for Graphite Epoxy, $\phi = 0$	29
16	Slowness Curve for Graphite Epoxy, $\phi = 30$	30
17	Skew Curve for Graphite Epoxy, $\phi = 30$	31
18	Slowness Curve for Quartz, $\phi = 0$, ($X - Z$ Plane)	32
19	Skew Curve for Quartz, $\phi = 0$, ($X - Z$ Plane)	33
20	Slowness Curve for Quartz, $\phi = 90$, ($Y - Z$ Plane)	34
21	Skew Curve for Quartz, $\phi = 90$, ($Y - Z$ Plane)	35
22	Slowness Curve for Quartz, $\phi = 90$, ($X - Y$ Plane)	36

23	Skew Curve for Quartz, $\phi = 90$, ($X - Y$ Plane)	37
24	Slowness Curve for CdS, $\phi = 0$, ($X - Y$ Plane)	38
25	Skew Curve for CdS, $\phi = 0$, ($X - Y$ Plane)	39
26	Slowness Curve for CdS, $\phi = 90$, ($X - Z$ Plane)	40
27	Skew Curve for CdS, $\phi = 90$, ($X - Z$ Plane)	41

1 Basic Equations

The dynamic behaviour of a linear elastic generally anisotropic solid can be conveniently expressed using tensorial notation as shown below in equation (1), where indices i and j vary over 1,2,3. The usual tensor summation convention is assumed¹

$$\frac{\partial \sigma'_{ij}}{\partial x'_j} = \rho' \frac{\partial^2 u'_i}{\partial t^2} \quad (1)$$

Equation (1), is written in the reference orthogonal coordinate system $x'_i = (x'_1, x'_2, x'_3)$. The constitutive relations, which show the interdependence of strain (ϵ'_{kl}) and stress ($\sigma'_{i,j}$) can be given either in terms of stiffnesses (c'_{ijkl})

$$\sigma'_{i,j} = c'_{ijkl} \epsilon'_{kl} \quad (2)$$

or inversely in terms of compliances (s'_{ijkl}) as in equation (3).

$$\epsilon'_{i,j} = s'_{ijkl} \sigma'_{kl} \quad (3)$$

Finally, strain and displacement (u'_i) are related as shown in equation (4).

$$\epsilon'_{k,l} = \frac{1}{2} \left(\frac{\partial u'_l}{\partial x'_k} + \frac{\partial u'_k}{\partial x'_l} \right). \quad (4)$$

In all of these equations, the presence of the prime indicates that the quantities are defined in the reference coordinate system.

Symmetry arguments allow some simplification of the quantities just introduced. The strain and stress tensors are symmetric, i.e. $\sigma'_{ij} = \sigma'_{ji}$ and $\epsilon'_{ij} = \epsilon'_{ji}$. Thus, the stiffness (and compliance tensors must have a corresponding degree of symmetry which leads to the simplifications shown in equation (5).

$$c'_{ijkl} = c'_{jikl} = c'_{ijlk} = c'_{jilk} \quad (5)$$

¹Summation over repeated indices: $x_{i,j}y_j = x_{i,1}y_1 + x_{i,2}y_2 + x_{i,3}y_3$.

By energy considerations, as demonstrated in Nayfeh [6] and Auld [1], it can be shown that there is further symmetry in the stiffness and compliance tensor. The argument begins with a definition of strain energy density, U , and the use of the constitutive relation (2).

$$U = \frac{1}{2} \sigma'_{ij} \epsilon'_{ij} = \frac{1}{2} c'_{ijkl} \epsilon'_{kl} \epsilon'_{ij} \quad (6)$$

Differentiating this expression gives the result

$$c'_{ijkl} = \frac{\partial^2 U}{\partial \epsilon'_{ij} \partial \epsilon'_{kl}}. \quad (7)$$

Interchanging the order of differentiation does not change this relation, and we conclude that

$$c'_{ijkl} = c'_{klij} \quad (8)$$

The simplifications introduced by (5) and (8) mean that rather than having $3 \times 3 \times 3 \times 3 = 81$ independent values, c'_{ijkl} has at most 21 independent coefficients.

2 Reduced Notation

Often, when writing out expressions involving material stiffness properties, it is convenient to use a reduced notation which takes advantage of the symmetry present in the stiffness tensors describing even the most general elastic materials. This notation is a convenience, and is widely used in books and papers. In short, the contractions are as follows, where each pair of subscripts in the tensor equations is mapped to a single subscript in the reduced equations:

$$\begin{aligned} 1 &\iff 11, & 2 &\iff 22, & 3 &\iff 33 \\ 4 &\iff 23, & 5 &\iff 13, & 6 &\iff 12 \end{aligned} \quad (9)$$

To facilitate the use of this notation, engineering shear strain is introduced, defined as follows:

$$\gamma'_{12} = 2\epsilon'_{12}, \quad \gamma'_{13} = 2\epsilon'_{13}, \quad \gamma'_{23} = 2\epsilon'_{23}, \quad (10)$$

We can now rewrite equation (2), using this new notation as shown in equation (11) (following the lead from Nayfeh [6], upper case C_{ij} is used to make the

distinction from the full notation c_{ijkl} more apparent).

$$\begin{bmatrix} \sigma'_{11} \\ \sigma'_{22} \\ \sigma'_{33} \\ \sigma'_{23} \\ \sigma'_{13} \\ \sigma'_{12} \end{bmatrix} = \begin{bmatrix} C'_{11} & C'_{12} & C'_{13} & C'_{14} & C'_{15} & C'_{16} \\ C'_{12} & C'_{22} & C'_{23} & C'_{24} & C'_{25} & C'_{26} \\ C'_{13} & C'_{23} & C'_{33} & C'_{34} & C'_{35} & C'_{36} \\ C'_{14} & C'_{24} & C'_{34} & C'_{44} & C'_{45} & C'_{46} \\ C'_{15} & C'_{25} & C'_{35} & C'_{45} & C'_{55} & C'_{56} \\ C'_{16} & C'_{26} & C'_{36} & C'_{46} & C'_{56} & C'_{66} \end{bmatrix} \begin{bmatrix} \epsilon'_{11} \\ \epsilon'_{22} \\ \epsilon'_{33} \\ \gamma'_{23} \\ \gamma'_{13} \\ \gamma'_{12} \end{bmatrix} \quad (11)$$

3 Material Symmetry

Up to this point, we have been dealing with the most general relationships applying to linear elastic, generally anisotropic materials. Such materials are referred to as triclinic materials. Many real materials have inherent symmetries which can greatly simplify their behaviour. In this section, we will look at some of these materials.

It is important to introduce the concept of transformation tensors. Transformations are fundamental to the definition of tensors. In general, a fourth order tensor such as c'_{ijkl} transforms from the reference coordinate system x'_i to an alternative coordinate system x_i as follows

$$c_{mnop} = \beta_{mi}\beta_{nj}\beta_{ok}\beta_{pl}c'_{ijkl}. \quad (12)$$

Similarly, a second order tensor such as the stress tensor σ'_{ij} transforms as follows.

$$\sigma_{mn} = \beta_{mi}\beta_{nj}\sigma'_{ij}. \quad (13)$$

Finally, a first order tensor such as the displacement tensor u'_i transforms simply as

$$u_m = \beta_{mi}u'_i. \quad (14)$$

The transformation tensor β_{ij} has as elements the cosines of the angles between the x_i and the x'_j axes.

We will define our various symmetry classes in terms of transformation tensors (e.g. for a mirror reflection, or a three fold rotation). A symmetry condition means that the stiffness (or compliance) tensor must be invariant under such a transformation. This allows the formulation of equations which lead to simplifications in the stiffness tensor, either through the elimination of entries, or the establishment of relations between them. This is the method shown in the following treatment.

A slightly different, alternative approach, used by Lekhnitskii [5], is to look at symmetry in terms of strain energy per unit volume, \bar{V} . Using the tensor summa-

tion convention, \bar{V} is shown in equation (15).

$$\bar{V} = \frac{1}{2} c_{ijkl} \sigma_{ij} \sigma_{kl} \quad (15)$$

Clearly, strain energy is independent of any particular coordinate system. If the material is symmetric under a coordinate transformation, then the terms c_{ijkl} of the stiffness tensor will also be invariant. The stresses σ_{ij} will transform to stresses σ'_{ij} in the new coordinate system. Applying these observations to equation (15) leads to the following result.

$$\frac{1}{2} c_{ijkl} \sigma_{ij} \sigma_{kl} = \frac{1}{2} c_{ijkl} \sigma'_{ij} \sigma'_{kl} \quad (16)$$

Given our earlier observations on the transformation of second order tensors (see equation (13)), we can easily substitute for the terms σ'_{ij} equivalent expressions in terms of the untransformed stresses, and the elements of the transformation matrix β_{ij} . Once this is done, coefficients for particular terms σ_{11} , σ_{12} , ... are equated and simplifications become apparent.

The field of crystallography is a large one, and it has developed a rigorous way of classifying and identifying symmetry classes. I will not attempt a full examination of material symmetry. I will, however, go so far as to include point group diagrams for most of the symmetry classes discussed. On these diagrams, points are marked using either crosses or circles. A cross indicates that a point is above the plane of the page, a circle indicates a point below the page. Under the transformations defining the symmetry class, all points shown on the diagram must be equivalent. In the naming of the groups, a number such as 2 or 3 indicates a 2 or 3 fold rotation axis. m indicates a plane of mirror symmetry. If we write, for example, $2/m$; this means that the plane of symmetry referred to by m is perpendicular to the axis referred to by 2. $2m$ would mean that the plane of mirror symmetry was parallel with the 2-fold rotation axis. An overbar, indicates that an inversion is applied (e.g. $\bar{2}$ indicates a 2-fold axis with inversion, $\bar{1}$ is a simple inversion).

We will see that materials having different point groups may in fact be equivalent in terms of their stiffness tensor symmetry requirements.

It should be noted that Nayfeh's book [6] simplifies greatly the discussion of symmetry. He gives only a single example of each class (equivalent to discussing only one point group). These notes originally (and perhaps to some extent still) reflect this simplification, though I am attempting to add more detail. Auld [1], Fedorov [2], and various books on crystallography [3, 4, 7] provide more thorough treatments of the area.

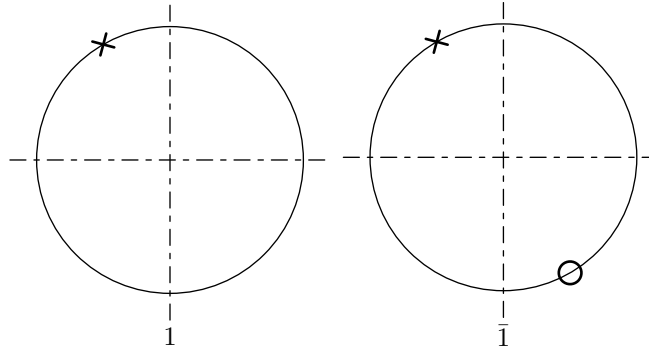


Figure 1: Triclinic Symmetry Point Groups

3.1 Triclinic Symmetry

It is worth noting that it is possible to introduce an inversion center without introducing any restrictions to the stiffness tensor. The transformation tensor for an inversion center is given as:

$$\beta_{ij} = \begin{bmatrix} -1 & 0 & 0 \\ 0 & -1 & 0 \\ 0 & 0 & -1 \end{bmatrix} \quad (17)$$

Now, since the stiffness tensor is even ordered (its order is 4), requiring identity under the application of β_{ij} to c_{ijkl} introduces no restrictions on the terms of c_{ijkl} . Similarly, in later discussion, any transformation tensors which differ only in terms of the application of an inversion center are equivalent in terms of their effects on the stiffness tensor.

It should also be noted that triclinic materials (and indeed all materials) are, of course, invariant under the identity operation.

3.2 Monoclinic Symmetry

Monoclinic materials are materials having, for example, one plane of mirror symmetry. Other examples can be seen in figure 19. Considering the mirror symmetry case, let us say that this plane coincides with the $x'_1 - x'_2$ plane. This symmetry condition requires that the material be invariant under the transformation β_{ij} defined by equation (18).

$$\beta_{ij} = \begin{bmatrix} 1 & 0 & 0 \\ 0 & 1 & 0 \\ 0 & 0 & -1 \end{bmatrix} \quad (18)$$

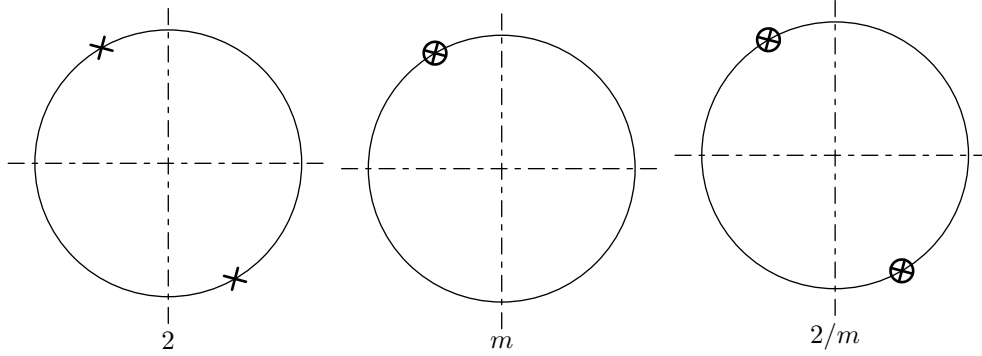


Figure 2: Monoclinic Symmetry Point Groups

Consider the formation of the term c_{2312} . Clearly $c_{2312} = \beta_{2i}\beta_{3i}\beta_{1i}\beta_{2i}c'_{ijkl}$. Now, looking at equation (18), it is clear that the terms $\beta_{ij} = 0$ for $i \neq j$. Thus we get $c_{2312} = \beta_{22}\beta_{33}\beta_{11}\beta_{22}c'_{2312} = -c'_{2312}$. However, we require that $c_{2312} = c'_{2312}$, which leads to the conclusion $c'_{2312} = 0$. Other elements of c'_{ijkl} which vanish are c'_{1123} , c'_{2223} , c'_{3323} , c'_{1113} , c'_{2213} , c'_{3313} and c'_{1312} . These are all the unique terms with an uneven number of 3's in their subscript. With these 8 terms removed, we are left with 13 unique coefficients (compared with 21 for the more general triclinic material). The form of the reduced stiffness matrix for monoclinic materials is shown in equation (19).

$$\begin{bmatrix} \sigma'_{11} \\ \sigma'_{22} \\ \sigma'_{33} \\ \sigma'_{23} \\ \sigma'_{13} \\ \sigma'_{12} \end{bmatrix} = \begin{bmatrix} C'_{11} & C'_{12} & C'_{13} & 0 & 0 & C'_{16} \\ C'_{12} & C'_{22} & C'_{23} & 0 & 0 & C'_{26} \\ C'_{13} & C'_{23} & C'_{33} & 0 & 0 & C'_{36} \\ 0 & 0 & 0 & C'_{44} & C'_{45} & 0 \\ 0 & 0 & 0 & C'_{45} & C'_{55} & 0 \\ C'_{16} & C'_{26} & C'_{36} & 0 & 0 & C'_{66} \end{bmatrix} \begin{bmatrix} \epsilon'_{11} \\ \epsilon'_{22} \\ \epsilon'_{33} \\ \gamma'_{23} \\ \gamma'_{13} \\ \gamma'_{12} \end{bmatrix} \quad (19)$$

3.3 Orthotropic Symmetry

If we introduce a second plane of symmetry, say the $x'_1 - x'_3$ plane, we get an orthotropic material. As well as being invariant under the transformation tensor (18), this material is also invariant under the transformation tensor (20).

$$\beta_{ij} = \begin{bmatrix} 1 & 0 & 0 \\ 0 & -1 & 0 \\ 0 & 0 & 1 \end{bmatrix} \quad (20)$$

Unique elements of c'_{ijkl} which vanish under this invariance condition are c'_{1112} , c'_{2212} , c'_{3312} and c'_{1323} (elements with even numbers of 2's). These simplifications leave us with $13 - 4 = 9$ independent coefficients. Since we have two orthogonal planes of symmetry, introducing a third plane will have no further effect on the stiffness tensor². The form of the reduced stiffness matrix for orthotropic ma-

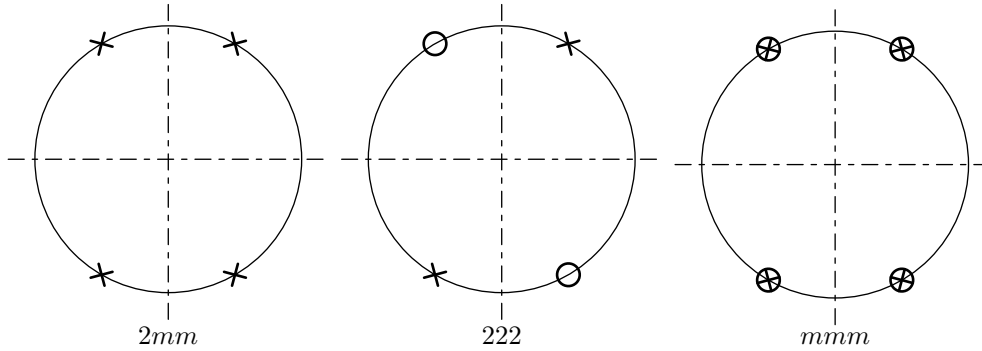


Figure 3: Orthotropic Symmetry Point Groups

terials is shown in equation (21). The point diagrams of the symmetry classes satisfied by this equation are shown in figure 3.

$$\begin{bmatrix} \sigma'_{11} \\ \sigma'_{22} \\ \sigma'_{33} \\ \sigma'_{23} \\ \sigma'_{13} \\ \sigma'_{12} \end{bmatrix} = \begin{bmatrix} C'_{11} & C'_{12} & C'_{13} & 0 & 0 & 0 \\ C'_{12} & C'_{22} & C'_{23} & 0 & 0 & 0 \\ C'_{13} & C'_{23} & C'_{33} & 0 & 0 & 0 \\ 0 & 0 & 0 & C'_{44} & 0 & 0 \\ 0 & 0 & 0 & 0 & C'_{55} & 0 \\ 0 & 0 & 0 & 0 & 0 & C'_{66} \end{bmatrix} \begin{bmatrix} \epsilon'_{11} \\ \epsilon'_{22} \\ \epsilon'_{33} \\ \gamma'_{23} \\ \gamma'_{13} \\ \gamma'_{12} \end{bmatrix} \quad (21)$$

3.4 Tetragonal Symmetry

In the next symmetry case, we introduce the concept of transformation by rotation. For the case of a counterclockwise rotation of an angle ϕ about the x'_3 axis, the

²Nayfeh [6] incorrectly states that if we have two perpendicular planes of mirror symmetry, then any plane normal to them must also be a plane of mirror symmetry. Working through the elementary calculations, we see that combining (18) and (20) does not produce the transformation matrix of the third plane of symmetry, but differs from it by a factor of -1 (it is equivalent to a two-fold rotation axis aligned along the intersection of the two mirror-planes). We have already seen (§3.1) that an inversion imposes no extra conditions on the stiffness matrix. Thus, Nayfeh is correct in ignoring the effect of a third plane of mirror symmetry on the stiffness tensor.

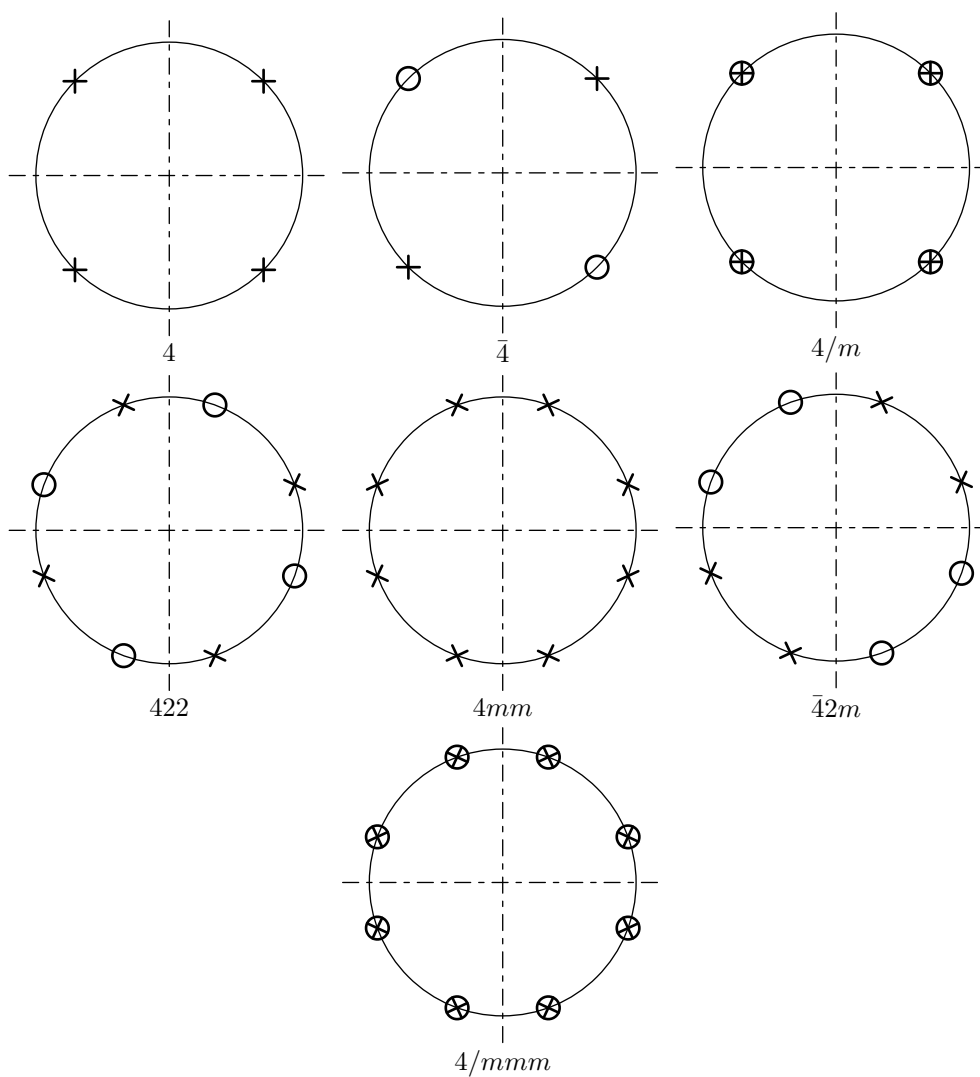


Figure 4: Tetragonal Symmetry Point Groups

transformation matrix β_{ij} is given as

$$\beta_{ij} = \begin{bmatrix} \cos \phi & \sin \phi & 0 \\ -\sin \phi & \cos \phi & 0 \\ 0 & 0 & 1 \end{bmatrix}. \quad (22)$$

Fedorov [2] describes the tetragonal symmetry class. In this case, we say that the material properties are invariant under rotations of $\phi = \pi/2$ about axis x'_3 . These systems have 6 significant elastic moduli³ The form of the reduced stiffness matrix for tetragonal materials is shown in equation (23).

$$\begin{bmatrix} \sigma'_{11} \\ \sigma'_{22} \\ \sigma'_{33} \\ \sigma'_{23} \\ \sigma'_{13} \\ \sigma'_{12} \end{bmatrix} = \begin{bmatrix} C'_{11} & C'_{12} & C'_{13} & 0 & 0 & 0 \\ C'_{12} & C'_{11} & C'_{13} & 0 & 0 & 0 \\ C'_{13} & C'_{13} & C'_{33} & 0 & 0 & 0 \\ 0 & 0 & 0 & C'_{44} & 0 & 0 \\ 0 & 0 & 0 & 0 & C'_{44} & 0 \\ 0 & 0 & 0 & 0 & 0 & C'_{66} \end{bmatrix} \begin{bmatrix} \epsilon'_{11} \\ \epsilon'_{22} \\ \epsilon'_{33} \\ \gamma'_{23} \\ \gamma'_{13} \\ \gamma'_{12} \end{bmatrix} \quad (23)$$

The matrix given in (23) is taken from Fedorov's work [2], and applies to all tetragonal materials. Auld [1] (and some Russian workers cited by Fedorov) divide the tetragonal (and trigonal, see below) systems into subclasses with either 7 or 6 independent moduli. The classes with 6 moduli have the matrix as shown in (23), while those with 7 have a matrix in the form of (24) below.

$$\begin{bmatrix} \sigma'_{11} \\ \sigma'_{22} \\ \sigma'_{33} \\ \sigma'_{23} \\ \sigma'_{13} \\ \sigma'_{12} \end{bmatrix} = \begin{bmatrix} C'_{11} & C'_{12} & C'_{13} & 0 & 0 & C'_{16} \\ C'_{12} & C'_{12} & C'_{13} & 0 & 0 & -C'_{16} \\ C'_{13} & C'_{13} & C'_{33} & 0 & 0 & 0 \\ 0 & 0 & 0 & C'_{44} & 0 & 0 \\ 0 & 0 & 0 & 0 & C'_{44} & 0 \\ C'_{16} & -C'_{16} & 0 & 0 & 0 & C'_{66} \end{bmatrix} \begin{bmatrix} \epsilon'_{11} \\ \epsilon'_{22} \\ \epsilon'_{33} \\ \gamma'_{23} \\ \gamma'_{13} \\ \gamma'_{12} \end{bmatrix} \quad (24)$$

The classes with 7 moduli are $4, \bar{4}$ and $4/m$. Those with 6 are $4mm, 422, \bar{4}2m$ and $4/mmm$. Fedorov asserts that the distinction is artificial, and that correct choice of axes reduces all tetragonal (and trigonal) systems to 6 independent significant

³Fedorov quotes different numbers of independent elastic moduli to Nayfeh, and also to Auld. For example, in the case of monoclinic crystal he gives the number of 12, as opposed to 13 in Nayfeh's work. As far as I understand, this discrepancy is because Fedorov uses the 13th number to fix the orientation of the coordinate system. Thus, for the orthorhombic/orthotropic system, Nayfeh and Fedorov agree on the number of 9, as the two perpendicular planes are sufficient to fix the orientation of the coordinate system. I should look into this in more detail, and maybe browse through a book on crystallography (Fedorov alludes to far more detail on symmetry classes than Nayfeh does).

moduli. It will be noted that the classes with the larger number of moduli are those which inherently fix only one direction (principally the axis about which the rotations occur), while the classes with 6 moduli are those which inherently fix all coordinate directions (axis of rotation, and normal to a mirror plane, for example). See also the footnote for a couple of notes. I will go through this in more detail in the future. The point groups for all of these classes are shown in figure 4.

3.5 Trigonal Symmetry

Materials with trigonal symmetry have a trigonal axis, which we will assume to coincide with x'_3 . This means that the material is invariant under rotations of $\phi = 2\pi/3$ about the x'_3 axis. According to Fedorov [2], in this case there are 6 significant moduli (see footnote in §3.4). The form of the reduced stiffness matrix for trigonal materials is shown in equation (25).

$$\begin{bmatrix} \sigma'_{11} \\ \sigma'_{22} \\ \sigma'_{33} \\ \sigma'_{23} \\ \sigma'_{13} \\ \sigma'_{12} \end{bmatrix} = \begin{bmatrix} C'_{11} & C'_{12} & C'_{13} & C'_{14} & -C'_{25} & 0 \\ C'_{12} & C'_{11} & C'_{13} & -C'_{14} & C'_{25} & 0 \\ C'_{13} & C'_{13} & C'_{33} & 0 & 0 & 0 \\ C'_{14} & -C'_{14} & 0 & C'_{44} & 0 & C'_{25} \\ -C'_{25} & C'_{25} & 0 & 0 & C'_{44} & C'_{14} \\ 0 & 0 & 0 & C'_{25} & C'_{14} & \frac{1}{2}(C'_{11} - C'_{12}) \end{bmatrix} \begin{bmatrix} \epsilon'_{11} \\ \epsilon'_{22} \\ \epsilon'_{33} \\ \gamma'_{23} \\ \gamma'_{13} \\ \gamma'_{12} \end{bmatrix} \quad (25)$$

Fedorov shows that equation (25) may be simplified by correct choice of coordinate system, to give the form:

$$\begin{bmatrix} \sigma'_{11} \\ \sigma'_{22} \\ \sigma'_{33} \\ \sigma'_{23} \\ \sigma'_{13} \\ \sigma'_{12} \end{bmatrix} = \begin{bmatrix} C'_{11} & C'_{12} & C'_{13} & C'_{14} & 0 & 0 \\ C'_{12} & C'_{11} & C'_{13} & -C'_{14} & 0 & 0 \\ C'_{13} & C'_{13} & C'_{33} & 0 & 0 & 0 \\ C'_{14} & -C'_{14} & 0 & C'_{44} & 0 & 0 \\ 0 & 0 & 0 & 0 & C'_{44} & C'_{14} \\ 0 & 0 & 0 & 0 & C'_{14} & \frac{1}{2}(C'_{11} - C'_{12}) \end{bmatrix} \begin{bmatrix} \epsilon'_{11} \\ \epsilon'_{22} \\ \epsilon'_{33} \\ \gamma'_{23} \\ \gamma'_{13} \\ \gamma'_{12} \end{bmatrix} \quad (26)$$

As mentioned before in section 3.4, Fedorov [2] and Auld [1] differ on the number of independent moduli. Fedorov asserts it is 6 for all trigonal classes. Auld argues that it is 7 for classes 3 and $\bar{3}$, which have the stiffness matrix as shown in (25). Auld says that there are 6 significant constants for classes 32, $3m$ and $\bar{3}m$. Similar arguments may be made as in the case of tetragonal systems 3.4. See also footnotes. More detail required on this topic. The point diagrams for all classes are shown in figure 5.

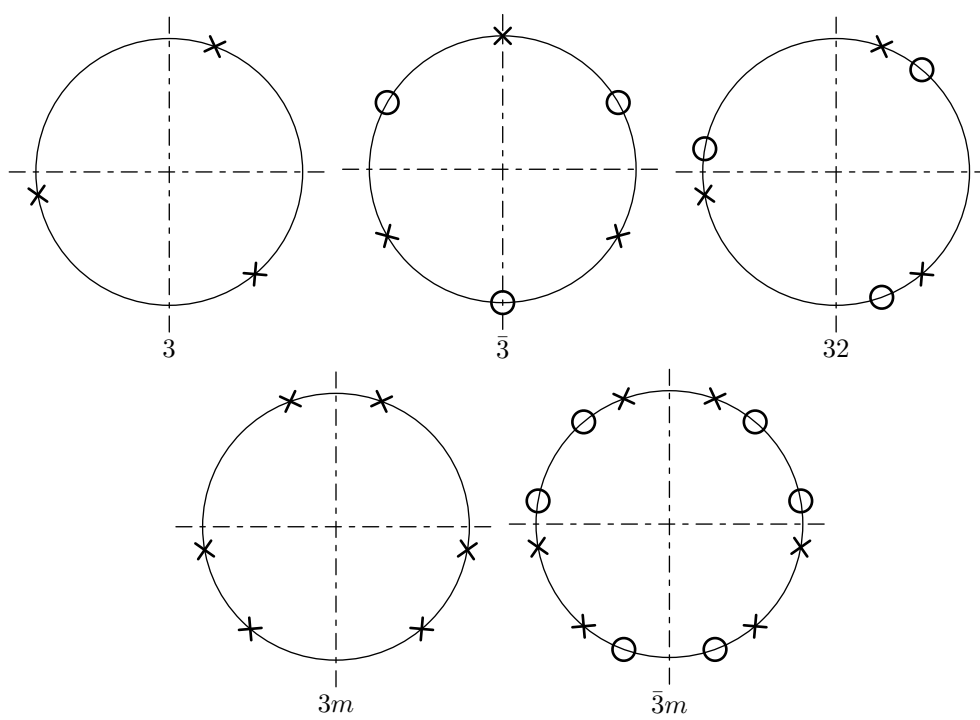


Figure 5: Trigonal Symmetry Point Groups

3.6 Transversely Isotropic Symmetry

To obtain properties for transversely isotropic materials, we can apply the rotation transformation (22) to the properties for an orthotropic material (see section 3.3). It is possible to write out expressions for each of the terms in the new stiffness tensor c_{ijkl} . Full details can be found in Nayfeh's book [6], and can also be found in the computer code accompanying this document. A couple of samples are presented here:

$$c_{1111} = c'_{1111} \cos^4 \phi + c'_{2222} \sin^4 \phi + 2(c'_{1122} + 2c'_{1212}) \sin^2 \phi \cos^2 \phi \quad (27)$$

$$c_{2222} = c'_{1111} \sin^4 \phi + c'_{2222} \cos^4 \phi + 2(c'_{1122} + 2c'_{1212}) \sin^2 \phi \cos^2 \phi \quad (28)$$

$$c_{2212} = (c'_{1111} - c'_{1122} - 2c'_{1212}) \cos \phi \sin^3 \phi + (c'_{1122} - c'_{2222} + 2c'_{1212}) \sin \phi \cos^3 \phi \quad (29)$$

Clearly from (27) and (28), if we require the material properties to be invariant for $\phi = \pi/2$, it is necessary for c'_{1111} and c'_{2222} to be identical. The full set of restrictions thus imposed are:

$$\begin{aligned} c'_{1111} &= c'_{2222} \\ c'_{2233} &= c'_{1133} \\ c'_{1313} &= c'_{2323} \end{aligned} \quad (30)$$

Further requiring invariance under general rotations about the x'_3 axis, leads to additional restrictions. Consider equation (29). Under the invariance condition, we require $c_{2212} = c'_{2212}$. However, for an orthotropic material, $c'_{2212} = 0$. This means that the right hand side of (29) equals zero. This, along with (30) gives the relation:

$$c'_{1111} - c'_{1122} = 2c'_{1212}. \quad (31)$$

Thus, there are $9 - 4 = 5$ independent coefficients in the stiffness tensor. The form of the reduced stiffness matrix for transversely isotropic materials is shown in equation (32). It should be noted that this appears to be identical to the matrix supplied by Fedorov [2] for the case of a hexagonal crystal. He forms the hexagonal case by noting that it is equivalent to the simultaneous presence of identically direct twofold and threefold axes. He forms the matrix C_{ij} for the hexagonal case by combining the properties of these two cases (equations (19) and (25)). The

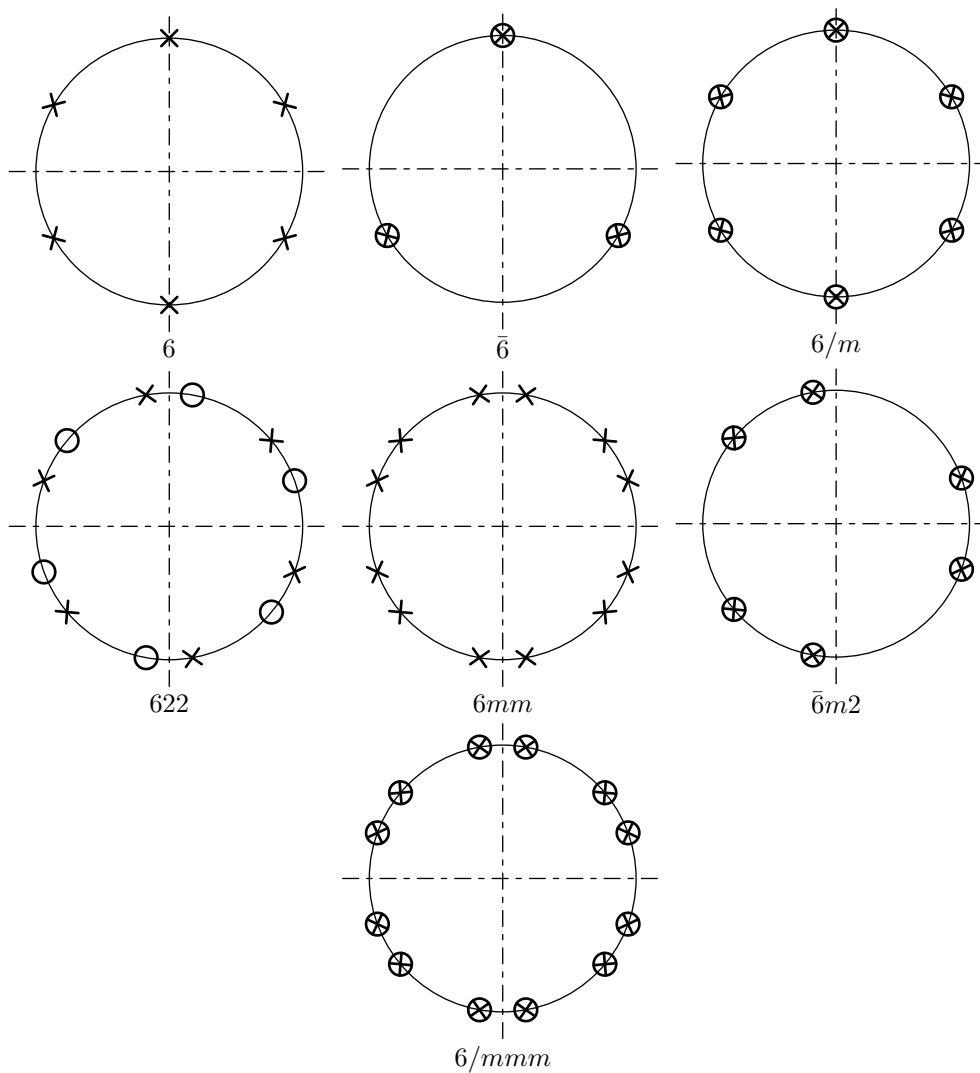


Figure 6: Hexagonal Symmetry Point Groups

point groups for the hexagonal symmetry case are shown in figure 6.

$$\begin{bmatrix} \sigma'_{11} \\ \sigma'_{22} \\ \sigma'_{33} \\ \sigma'_{23} \\ \sigma'_{13} \\ \sigma'_{12} \end{bmatrix} = \begin{bmatrix} C'_{11} & C'_{12} & C'_{13} & 0 & 0 & 0 \\ C'_{12} & C'_{11} & C'_{13} & 0 & 0 & 0 \\ C'_{13} & C'_{13} & C'_{33} & 0 & 0 & 0 \\ 0 & 0 & 0 & C'_{55} & 0 & 0 \\ 0 & 0 & 0 & 0 & C'_{55} & 0 \\ 0 & 0 & 0 & 0 & 0 & \frac{1}{2}(C'_{11} - C'_{12}) \end{bmatrix} \begin{bmatrix} \epsilon'_{11} \\ \epsilon'_{22} \\ \epsilon'_{33} \\ \gamma'_{23} \\ \gamma'_{13} \\ \gamma'_{12} \end{bmatrix} \quad (32)$$

3.7 Cubic Symmetry

To define cubic symmetry, we start from the orthotropic case (§3.3), and again apply rotations, both by angle ϕ about the x'_3 axis (as in §3.6) and by angle γ about the x'_2 axis. We require that the material is invariant for rotations $\phi = \pi/2$ and $\gamma = \pi/2$. This means that the coordinates x'_1 , x'_2 and x'_3 are completely interchangeable. This reduces by 6 the number of independent stiffness coefficients (compared with the orthotropic case) to give $9 - 6 = 3$ independent coefficients. The form of the reduced stiffness matrix for cubic isotropic materials is shown in equation (33).

$$\begin{bmatrix} \sigma'_{11} \\ \sigma'_{22} \\ \sigma'_{33} \\ \sigma'_{23} \\ \sigma'_{13} \\ \sigma'_{12} \end{bmatrix} = \begin{bmatrix} C'_{11} & C'_{12} & C'_{12} & 0 & 0 & 0 \\ C'_{12} & C'_{11} & C'_{12} & 0 & 0 & 0 \\ C'_{12} & C'_{12} & C'_{11} & 0 & 0 & 0 \\ 0 & 0 & 0 & C'_{66} & 0 & 0 \\ 0 & 0 & 0 & 0 & C'_{66} & 0 \\ 0 & 0 & 0 & 0 & 0 & C'_{66} \end{bmatrix} \begin{bmatrix} \epsilon'_{11} \\ \epsilon'_{22} \\ \epsilon'_{33} \\ \gamma'_{23} \\ \gamma'_{13} \\ \gamma'_{12} \end{bmatrix} \quad (33)$$

3.8 Isotropic Symmetry

Finally, the greatest degree of symmetry possible is isotropic symmetry. In this case, the material is invariant under rotation by arbitrary angles γ and ϕ . In this case, there are only two independent stiffness constants. The form of the reduced stiffness matrix for cubic isotropic materials is shown in equation (34) (stress and strain terms are omitted for clarity). Point group diagrams are superfluous for this case as every point is equivalent to every other point.

$$\begin{bmatrix} C'_{11} & C'_{12} & C'_{12} & 0 & 0 & 0 \\ C'_{12} & C'_{11} & C'_{12} & 0 & 0 & 0 \\ C'_{12} & C'_{12} & C'_{11} & 0 & 0 & 0 \\ 0 & 0 & 0 & \frac{1}{2}(C'_{11} - C'_{12}) & 0 & 0 \\ 0 & 0 & 0 & 0 & \frac{1}{2}(C'_{11} - C'_{12}) & 0 \\ 0 & 0 & 0 & 0 & 0 & \frac{1}{2}(C'_{11} - C'_{12}) \end{bmatrix} \quad (34)$$

4 Bulk Waves

4.1 Bulk Waves Background

In general, for wave propagation in a direction \vec{n} , three types of waves are possible. These are associated with the directions of the three particle displacement vectors $\vec{u}^{(k)}$ ($k = 1, 2, 3$). These can be referred to as having different polarisations. Pure modes can be defined in different ways, but Nayfeh [6] and Auld [1] define them as modes where either $\vec{u} \perp \vec{n}$ or $\vec{u} \parallel \vec{n}$. Where $\vec{u} \perp \vec{n}$, we say that the mode is longitudinal. Where $\vec{u} \parallel \vec{n}$, we can say that the mode is shear. In cases where the modes are not pure, they are described as quasi-longitudinal or quasi-shear, depending on which they are closest to.

Combining the momentum equation (1) and the stress-strain relation (2) and the strain-displacement relationship (4), gives the following result:

$$\rho \frac{\partial^2 u_i}{\partial t^2} = \frac{1}{2} c_{ijkl} \frac{\partial}{\partial x_j} \left(\frac{\partial u_l}{\partial x_k} + \frac{\partial u_k}{\partial x_l} \right) \quad (35)$$

By symmetry arguments (k and l are interchangeable) we can simplify (35) to get

$$\rho \frac{\partial^2 u_i}{\partial t^2} = c_{ijkl} \frac{\partial^2 u_l}{\partial x_k \partial x_j} \quad (36)$$

We look for solutions, u_i of the following form, in terms of ζ the bulk wavenumber, \vec{U} the displacement amplitude vector (which defines polarisation), and \vec{n} the propagation direction unit vector:

$$u_i = U_i e^{j(\zeta n_j x_j - \omega t)} \quad (37)$$

Substituting (37) into (36), and introducing $\lambda_{ijkl} = c_{ijkl} / \rho$, gives the following:

$$\omega^2 U_i = \frac{c_{ijkl}}{\rho} \zeta^2 n_k n_j U_l \Leftrightarrow \omega^2 U_i = \lambda_{ijkl} \zeta^2 n_k n_j U_l \quad (38)$$

Now, we introduce the phase velocity, v , defined as follows:

$$v = \frac{\omega}{\zeta} \quad (39)$$

Using v , equation (38) can be rewritten as follows:

$$\begin{aligned} & \left(\lambda_{ijkl} n_k n_j - v^2 \delta_{il} \right) U_l = 0 \\ \Leftrightarrow & \left(\Lambda_{il} - v^2 \delta_{il} \right) U_l = 0 \end{aligned} \quad (40)$$

where $\Lambda_{il} = \lambda_{ijkl} n_k n_j$. Clearly (40) represents an eigenvalue problem, where the phase velocities v are the eigenvalues, and the U_l vectors (polarisation vectors) are the eigenvectors. In general, there will be three phase velocities, accompanied by three polarisation vectors. These phase velocities and polarisations define a single (quasi)longitudinal and two (quasi)shear modes. Explicitly, the eigenvalue problem is as follows

$$\begin{pmatrix} \Lambda_{11} - v^2 & \Lambda_{12} & \Lambda_{13} \\ \Lambda_{12} & \Lambda_{22} - v^2 & \Lambda_{23} \\ \Lambda_{13} & \Lambda_{23} & \Lambda_{33} - v^2 \end{pmatrix} \begin{Bmatrix} U_1 \\ U_2 \\ U_3 \end{Bmatrix} = 0 \quad (41)$$

An important concept to introduce at this stage is the *slowness curve*. A slowness curve is a plot of the inverse of velocity (units are therefore seconds/metre or equivalent). Typically, a slowness curve is produced by choosing a plane in the material of interest, and then calculating the different phase velocities for a selection of propagation directions. Slowness is then plotted as a function of propagation direction in a polar plot. Slowness curves feature in most texts dealing with wave propagation in solids. Slowness curves can be combined to obtain a slowness surface, which would completely characterise the phase velocities of the possible modes in a given material. However, there are obvious difficulties in printing or displaying such surfaces.

Another concept which is introduced is the *skew curve*. This is a plot which I have only seen in Nayfeh's work [6]. As was mentioned earlier (page 17), pure modes are defined as being modes which are either normal to or parallel with the direction of propagation. Skew is a measure of how far any particular mode deviates from this ideal. If the mode is pure, skew will be zero. For other modes, the skew is the angle between the polarisation vector and the direction of propagation (for quasi-longitudinal modes) or the normal to the direction of propagation (for quasi-shear modes).

4.2 Computation of Slowness and Skew Curves Background

At this point, we are ready to calculate slowness curves for a wide range of materials. All that is required are the entries from the stiffness tensor c_{ijkl} , or equivalently the entries of the reduced stiffness matrix C_{ij} .

We map out the slowness data by considering planes parallel to the x_3 axis

(which without loss of generality, can coincide with the x'_3 axis). Given a set of material properties c'_{ijkl} , expressed in the coordinate system (x'_1, x'_2, x'_3) , we can transform it to c_{ijkl} expressed in the coordinate system (x_1, x_2, x_3) by rotating about the x'_3 axis. In this way, we can arrange that the coordinates of any direction of propagation, \vec{n} are of the form

$$\vec{n} = \begin{Bmatrix} \cos \theta \\ 0 \\ \sin \theta \end{Bmatrix} \quad \text{where} \quad 0 \leq \theta \leq 2\pi \quad (42)$$

when expressed in the transformed coordinate system. Once the transformed stiffness matrix or tensor is obtained, the angle θ is varied in the range $0 \leq \theta \leq 2\pi$, giving different propagation direction vectors, \vec{n} . For each \vec{n} , Λ_{ij} from equation (41) is obtained. The eigenvalues and eigenvectors of Λ_{ij} are found. The entire slowness surface can be determined by applying different rotations about x_3 and repeating the process.

An issue that caused me some difficulty when implementing this code was the sorting of the modes (i.e. which eigenvector/eigenvalue pair corresponds to longitudinal mode, which corresponds to the “fast shear” mode and which corresponds to the “slow shear” mode). Sorting by phase velocity gives correct results in particular cases, but for some materials the slowness curves cross each other (we will see this shortly). Nayfeh [6] indicates that the modes can be identified by looking at the dot and cross products of their eigenvectors with the propagation direction \vec{n} . This immediately identifies the longitudinal mode, which will generally make a relatively small angle with the propagation direction. The two remaining shear modes can then be sorted by how close they come to being normal to the propagation direction. For some cases this is sufficient to sort the modes. However for other more complicated materials, this leads to “curve-jumping”. An alternative tried was to sort the shear modes by how close they came to lying along the x_2 axis (i.e. to being perpendicular to the plane containing the x_3 axis and the propagation directions. Again, this works for some materials, but at particular points the modes swap over leading to discontinuities in the curves.

The solution I settled on when sorting the modes is as follows. For the first propagation direction tested, take the dot product of each polarisation vector with the propagation direction. The vector giving the largest number (smallest angle) is designated as the quasi-longitudinal mode. Then take the dot product of the remaining two vectors with the vector $(0, 1, 0)$. The mode giving the largest dot-product is designated as the first shear mode. The remaining mode is the second shear mode. For subsequent propagation directions \vec{n} , classify the resulting eigenvectors by how close they come to the previous longitudinal or shear modes (again using dot products). This works as long as each \vec{n} is relatively close to the previous

one (i.e. as long as the increments in θ are relatively small). In this way, the new vector closest to our last longitudinal vector is the new longitudinal mode. The new vector closest to the previous first shear mode vector is the new first shear mode. The remaining vector is the new second shear mode.

4.3 Examples of Slowness and Skew Curves

In this section I will present some sample slowness and skew curves calculated with the Python code I have written. Material properties used will also be presented here. The examples chosen are the same as the ones used by Nayfeh, so that I could more easily verify their correctness.

4.3.1 Aluminium

Aluminium is an isotropic material (this is not true in all cases, for example rolled aluminium can have directionality in material properties), and has very simple slowness and skew curves. The propagation velocities are the same for all directions. Skew is zero for all directions (all modes are pure modes). Additionally, the two shear modes present are degenerate (they have the same velocity). The slowness curve is shown in figure 7. The material properties are shown in equation 43.

$$\begin{bmatrix} 107.50 & 54.59 & 54.59 & 0.00 & 0.00 & 0.00 \\ 54.59 & 107.50 & 54.59 & 0.00 & 0.00 & 0.00 \\ 54.59 & 54.59 & 107.50 & 0.00 & 0.00 & 0.00 \\ 0.00 & 0.00 & 0.00 & 26.45 & 0.00 & 0.00 \\ 0.00 & 0.00 & 0.00 & 0.00 & 26.45 & 0.00 \\ 0.00 & 0.00 & 0.00 & 0.00 & 0.00 & 26.45 \end{bmatrix} \quad (43)$$

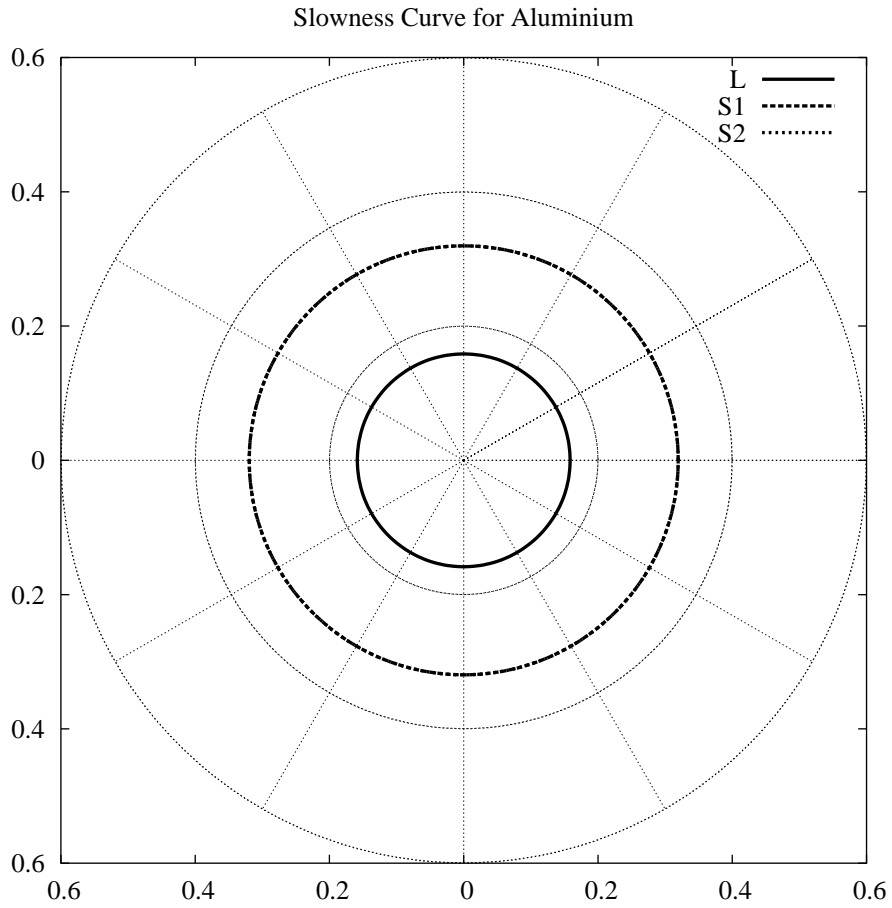
4.3.2 InAs

InAs is a cubic material. Its reduced stiffness matrix is given below for coordinate axes coinciding with cubic axes (i.e. in its simplest form).

$$\begin{bmatrix} 83.29 & 45.26 & 45.26 & 0.0 & 0.0 & 0.0 \\ 45.26 & 83.29 & 45.26 & 0.0 & 0.0 & 0.0 \\ 45.26 & 45.26 & 83.29 & 0.0 & 0.0 & 0.0 \\ 0.0 & 0.0 & 0.0 & 39.59 & 0.0 & 0.0 \\ 0.0 & 0.0 & 0.0 & 0.0 & 39.59 & 0.0 \\ 0.0 & 0.0 & 0.0 & 0.0 & 0.0 & 39.59 \end{bmatrix} \quad (44)$$

This gives the slowness and skew curves as shown below in figures 8 and 9.

Figure 7: Slowness Curve for Isotropic Aluminium



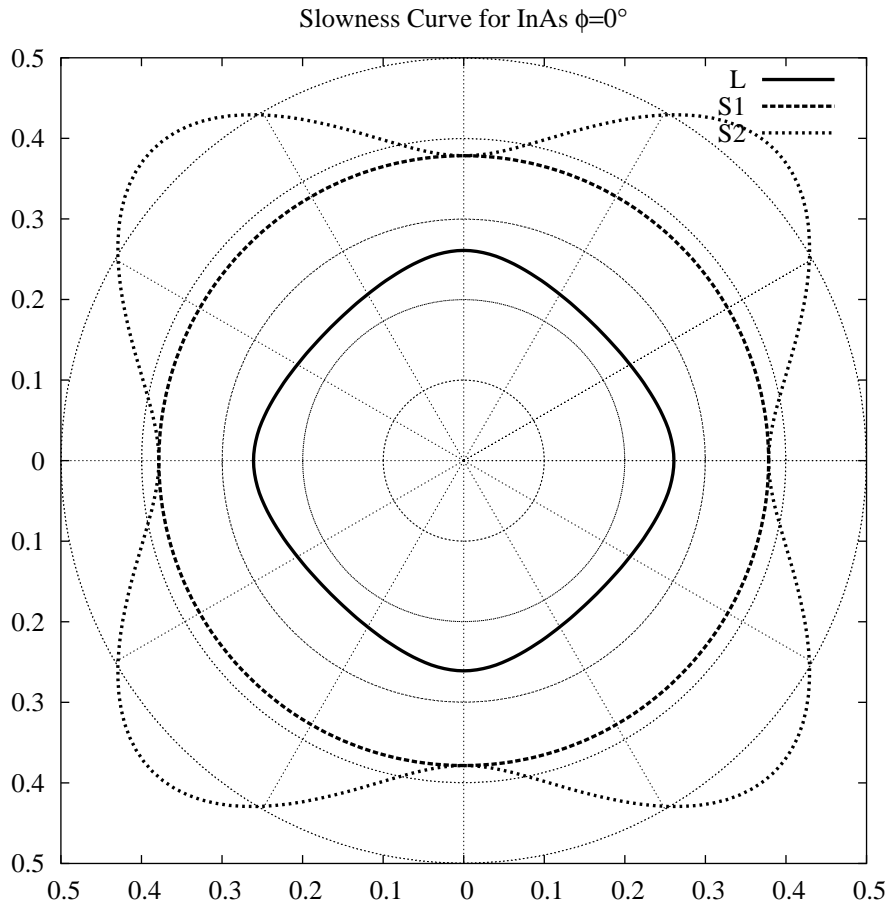
Rotating by an angle of 45 gives the reduced stiffness matrix shown in (45).

$$\begin{bmatrix}
 103.86 & 24.68 & 45.26 & 0.0 & 0.0 & 0.0 \\
 24.68 & 103.86 & 45.26 & 0.0 & 0.0 & 0.0 \\
 45.26 & 45.26 & 83.29 & 0.0 & 0.0 & 0.0 \\
 0.0 & 0.0 & 0.0 & 39.59 & 0.0 & 0.0 \\
 0.0 & 0.0 & 0.0 & 0.0 & 39.59 & 0.0 \\
 0.0 & 0.0 & 0.0 & 0.0 & 0.0 & 19.01
 \end{bmatrix} \quad (45)$$

Computation of the slowness and skew curves is straightforward. They are plotted in figures 10 and 11 respectively.

Rotating by an angle of 30 degrees (relative to the *original* orientation repre-

Figure 8: Slowness Curve for InAs, $\phi = 0$

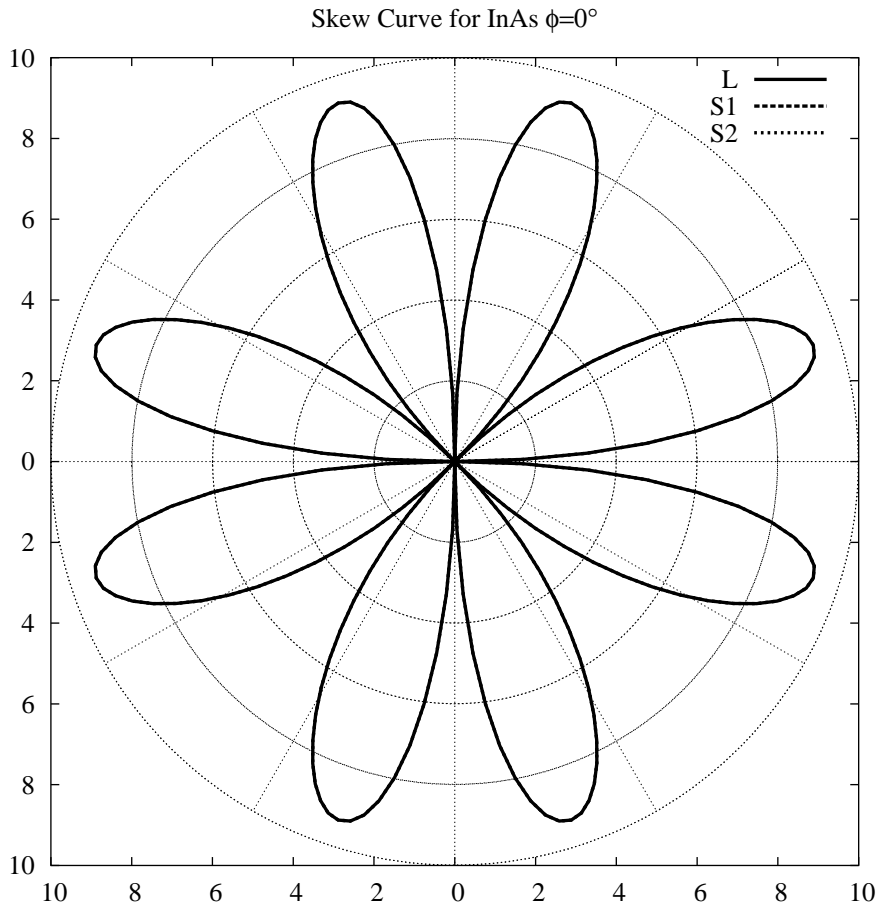


sented by (44)) gives the reduced stiffnes matrix of (46).

$$\begin{bmatrix} 98.72 & 29.83 & 45.26 & 0.00 & 0.00 & -8.91 \\ 29.83 & 98.72 & 45.26 & 0.00 & 0.00 & 8.91 \\ 45.26 & 45.26 & 83.29 & 0.00 & 0.00 & 0.00 \\ 0.00 & 0.00 & 0.00 & 39.59 & 0.00 & 0.00 \\ 0.00 & 0.00 & 0.00 & 0.00 & 39.59 & 0.00 \\ -8.91 & 8.91 & 0.00 & 0.00 & 0.00 & 24.16 \end{bmatrix} \quad (46)$$

The computed slowness and skew curves are shown in figures 12 and 13 respectively.

Figure 9: Skew Curve for InAs, $\phi = 0$



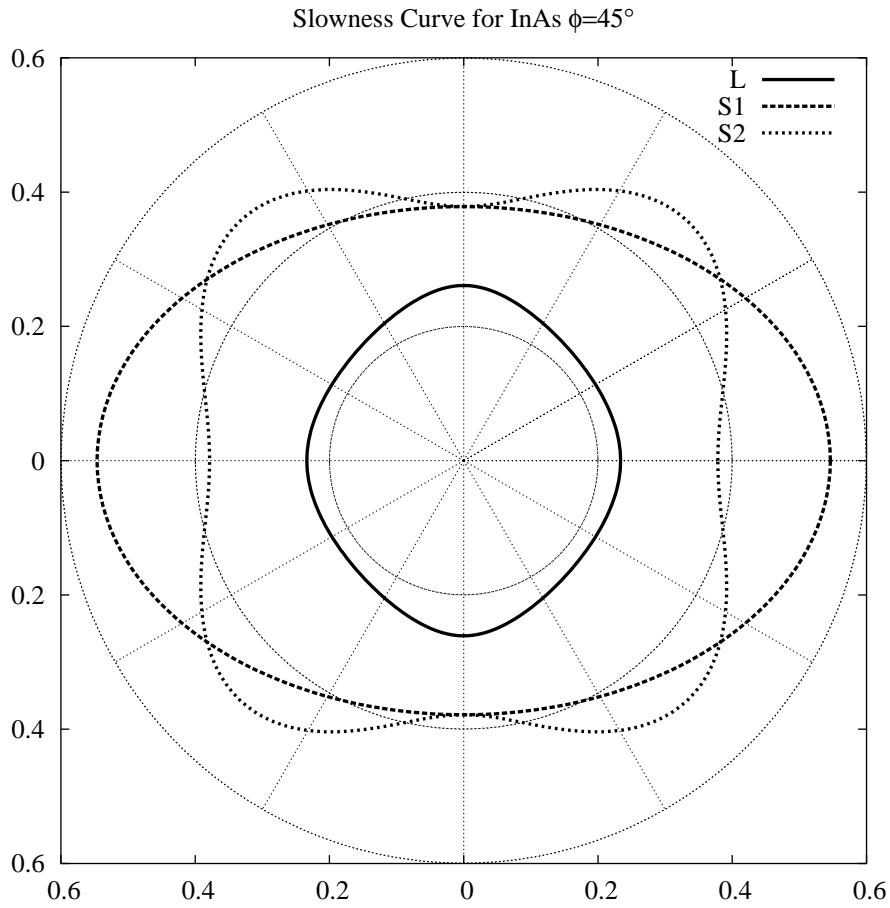
4.3.3 Graphite-Epoxy (65%-35%)

First, it should be noted that these curves differ significantly from those given by Nayfeh. There is at least one error in the material properties provided by Nayfeh⁴ Graphite-epoxy slowness and skew curves are shown in figures 14 and

⁴If I remember correctly, the Graphite-Epoxy $\phi = 30$ data cannot be obtained from the $\phi = 0$ data through transformation relations. Rather, it differs in a couple of terms by a factor of -1. The material properties given here are taken directly from the ones provided by Nayfeh, errors and all, though I may correct them in the future when I know which data are correct. I will soon begin reproducing figures from Auld for further validation of this code.

Note on Tue Jun 18 15:50:35 IST 2002: I have done this for quartz, a trigonal material, in § 4.3.4.

Figure 10: Slowness Curve for InAs, $\phi = 45^\circ$

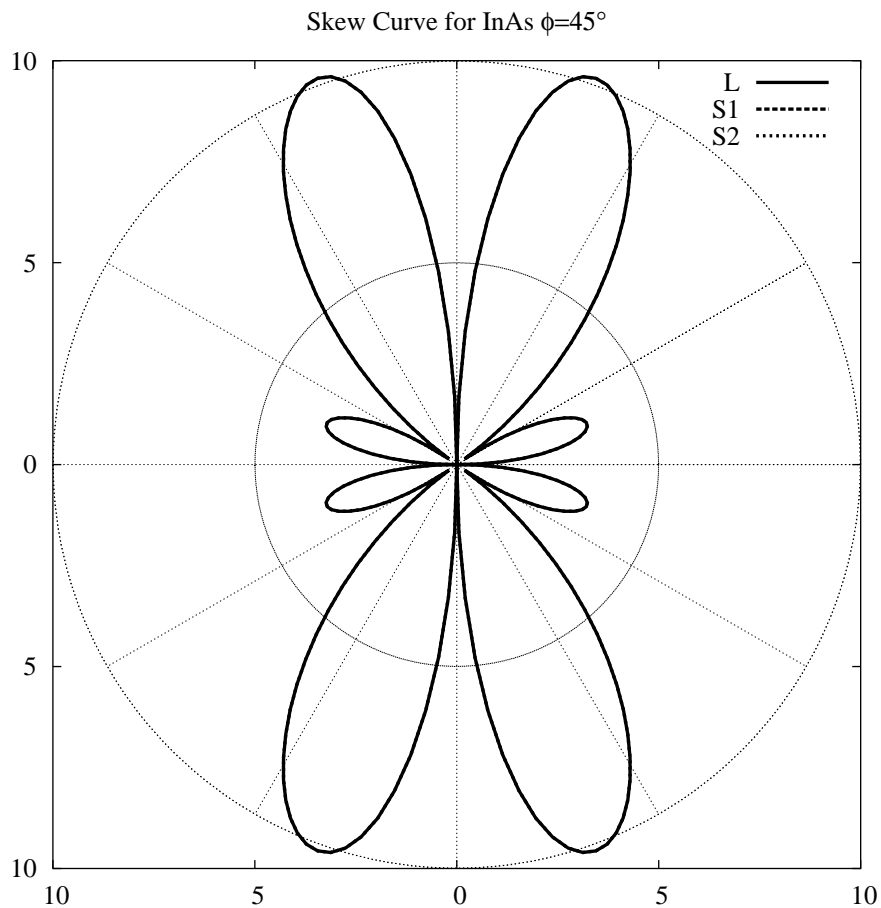


15 respectively. The matrix of stiffness constants is shown in equation (47).

$$\begin{bmatrix}
 155.43 & 3.72 & 3.72 & 0.00 & 0.00 & 0.00 \\
 3.72 & 16.34 & 4.96 & 0.00 & 0.00 & 0.00 \\
 3.72 & 4.96 & 16.34 & 0.00 & 0.00 & 0.00 \\
 0.00 & 0.00 & 0.00 & 3.37 & 0.00 & 0.00 \\
 0.00 & 0.00 & 0.00 & 0.00 & 7.48 & 0.00 \\
 0.00 & 0.00 & 0.00 & 0.00 & 0.00 & 7.48
 \end{bmatrix} \quad (47)$$

Corresponding slowness and skew curves for graphite-epoxy after a 30 degrees rotation are shown in figures 16 and 17. The matrix of material properties following

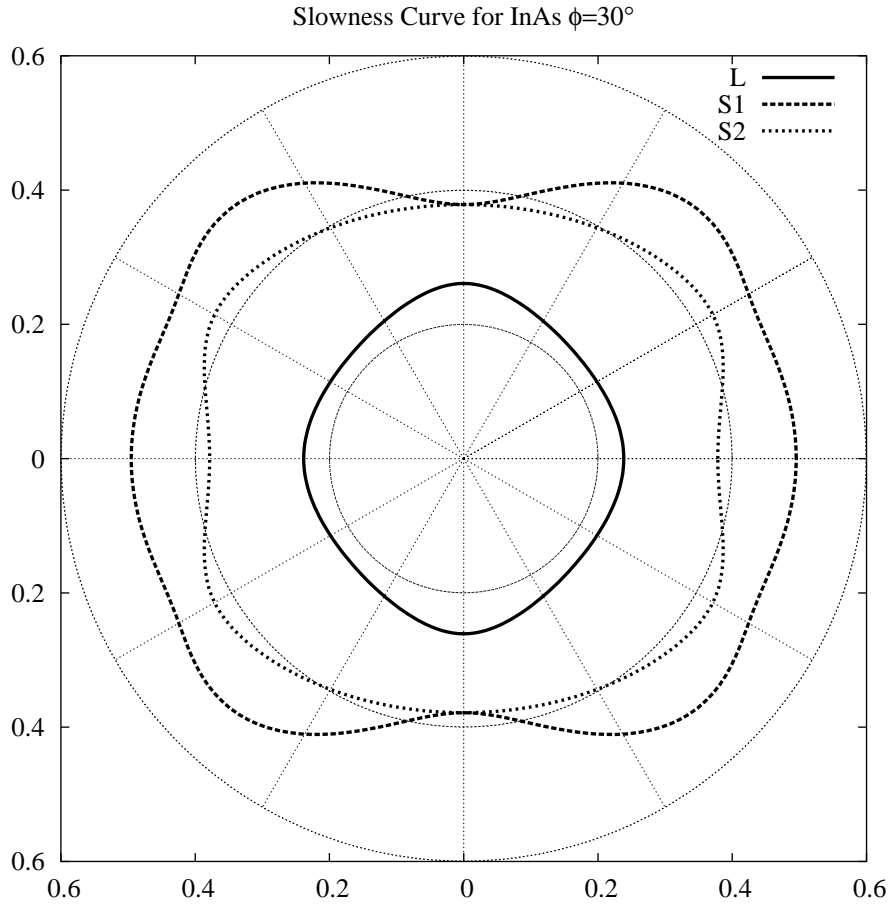
Figure 11: Skew Curve for InAs, $\phi = 45^\circ$



this transformation are show in (48).

$$\begin{bmatrix}
 95.46 & 28.93 & 4.03 & 0.00 & 0.00 & 44.67 \\
 28.93 & 25.91 & 4.65 & 0.00 & 0.00 & 15.56 \\
 4.03 & 4.65 & 16.34 & 0.00 & 0.00 & 0.54 \\
 0.00 & 0.00 & 0.00 & 4.40 & -1.78 & 0.00 \\
 0.00 & 0.00 & 0.00 & -1.78 & 6.45 & 0.00 \\
 44.67 & 15.56 & 0.54 & 0.00 & 0.00 & 32.68
 \end{bmatrix} \quad (48)$$

Figure 12: Slowness Curve for InAs, $\phi = 30$



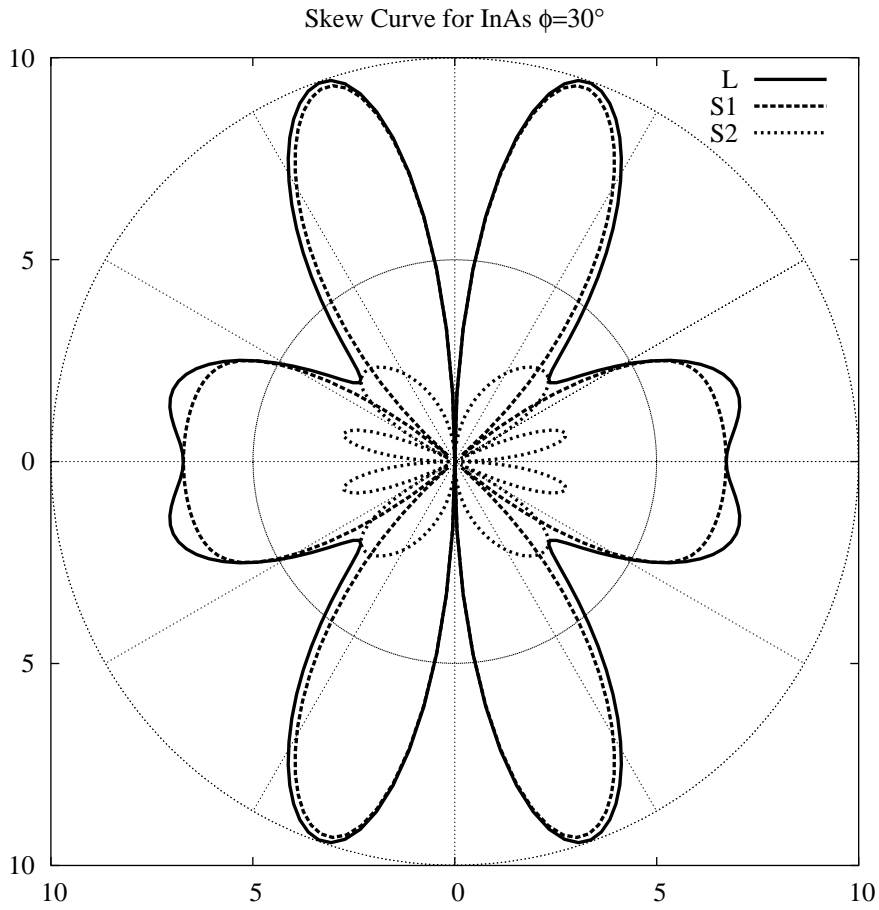
4.3.4 Quartz

First, it must be noted that in this discussion, the piezoelectric properties are neglected. The material properties given by Auld are as follows

$$\begin{aligned}
 c_{11} &= 8.674 \times 10^{10} \text{N/m}^2 & c_{12} &= 0.699 \times 10^{10} \text{N/m}^2 \\
 c_{33} &= 10.72 \times 10^{10} \text{N/m}^2 & c_{13} &= 0.699 \times 10^{10} \text{N/m}^2 \\
 c_{44} &= 5.794 \times 10^{10} \text{N/m}^2 & c_{14} &= -1.791 \times 10^{10} \text{N/m}^2
 \end{aligned}$$

Since quartz is a trigonal material, the remainder of the stiffness matrix can be determined by substituting into (26). Solving the eigenvalue problem for the slowness and skew of the different polarisations gives the results shown in figures 18

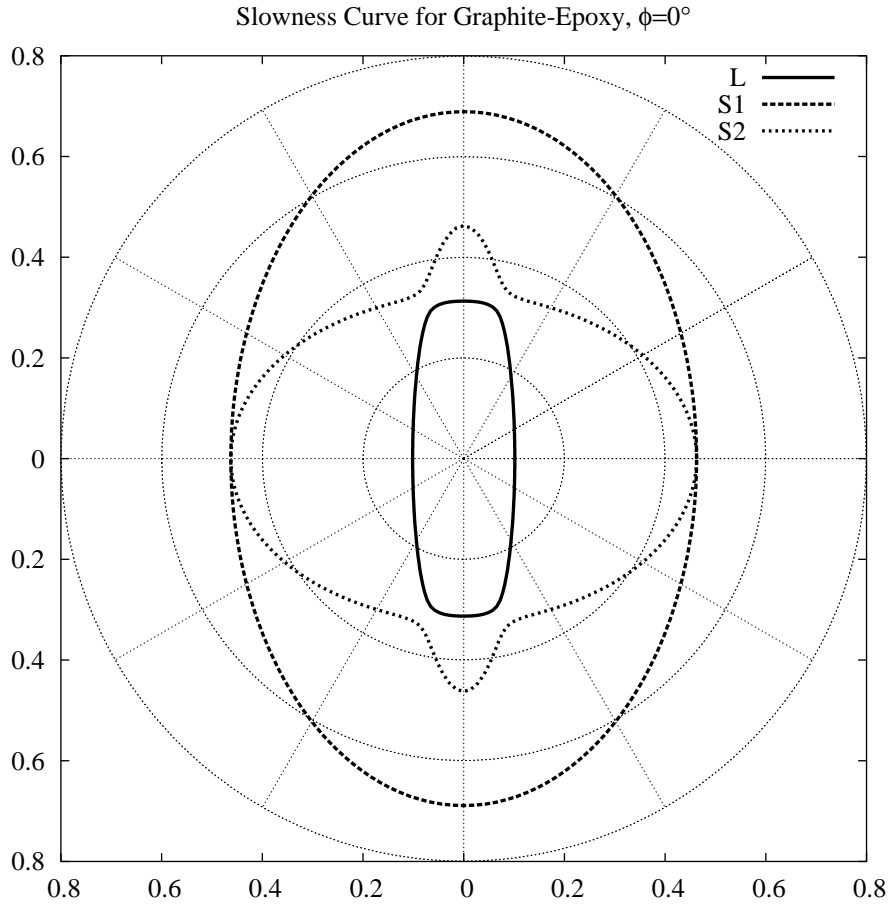
Figure 13: Skew Curve for InAs, $\phi = 30^\circ$



and 19. Applying a rotation of $\pi/2$ about the Z axis, gives the slowness and skew curves shown in figures 20 and 21.

We now look at propagation in the plane perpendicular to the Z axis. This means that we rotate the coordinates from the first system by $\pi/2$ about the X axis, or equivalently rotate the coordinates from the second system by $\pi/2$ about the Y axis. The resulting slowness and skew curves are shown in figures 22 and 23.

Figure 14: Slowness Curve for Graphite Epoxy, $\phi = 0$



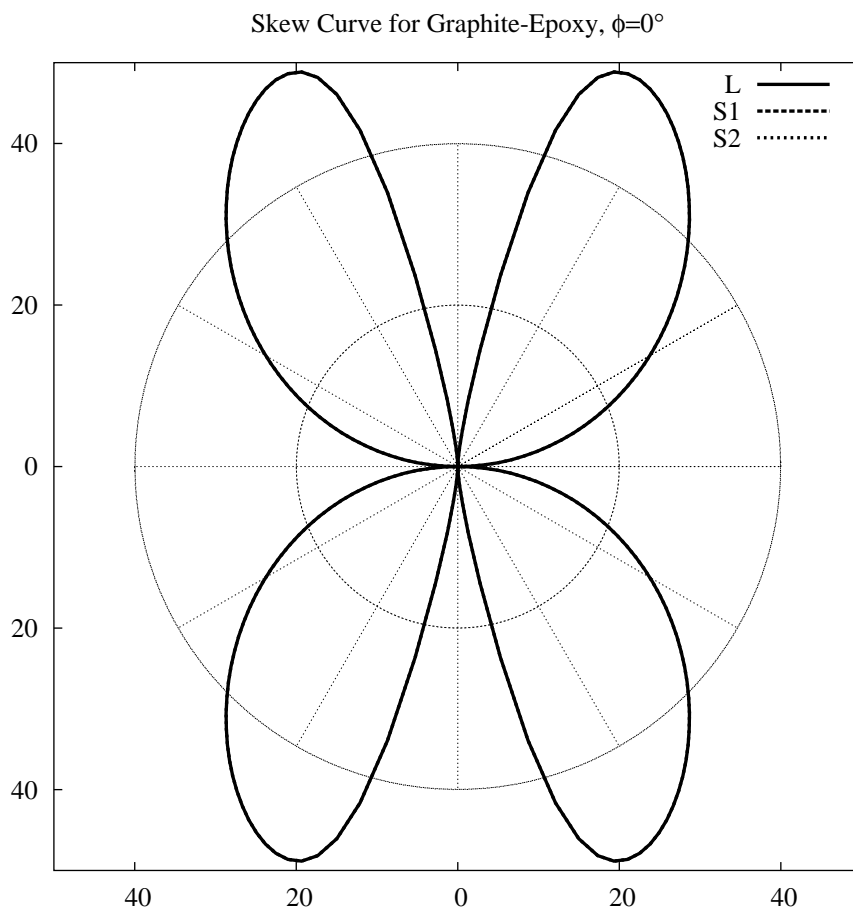
4.3.5 Cadmium Sulfide

Piezoelectric properties are neglected in this case. The material properties given by Auld are as follows

$$\begin{aligned}
 c_{11} &= 9.07 \times 10^{10} \text{N/m}^2 & c_{12} &= 5.81 \times 10^{10} \text{N/m}^2 \\
 c_{33} &= 9.38 \times 10^{10} \text{N/m}^2 & c_{13} &= 5.10 \times 10^{10} \text{N/m}^2 \\
 c_{44} &= 1.504 \times 10^{10} \text{N/m}^2
 \end{aligned}$$

Since cadmium sulfide is a hexagonal material, the remainder of the stiffness matrix can be determined by substituting into (32). Solving the eigenvalue problem for the slowness and skew of the different polarisations gives the results shown

Figure 15: Skew Curve for Graphite Epoxy, $\phi = 0$



in figures 24 and 25. This is for propagation in the plane normal to the axis of symmetry. Rotating the coordinate system by $\pi/2$ and again solving the eigenvalue problem gives the results for a plane parallel to the axis of symmetry. These results are shown in figures 26 and 27.

Figure 16: Slowness Curve for Graphite Epoxy, $\phi = 30^\circ$

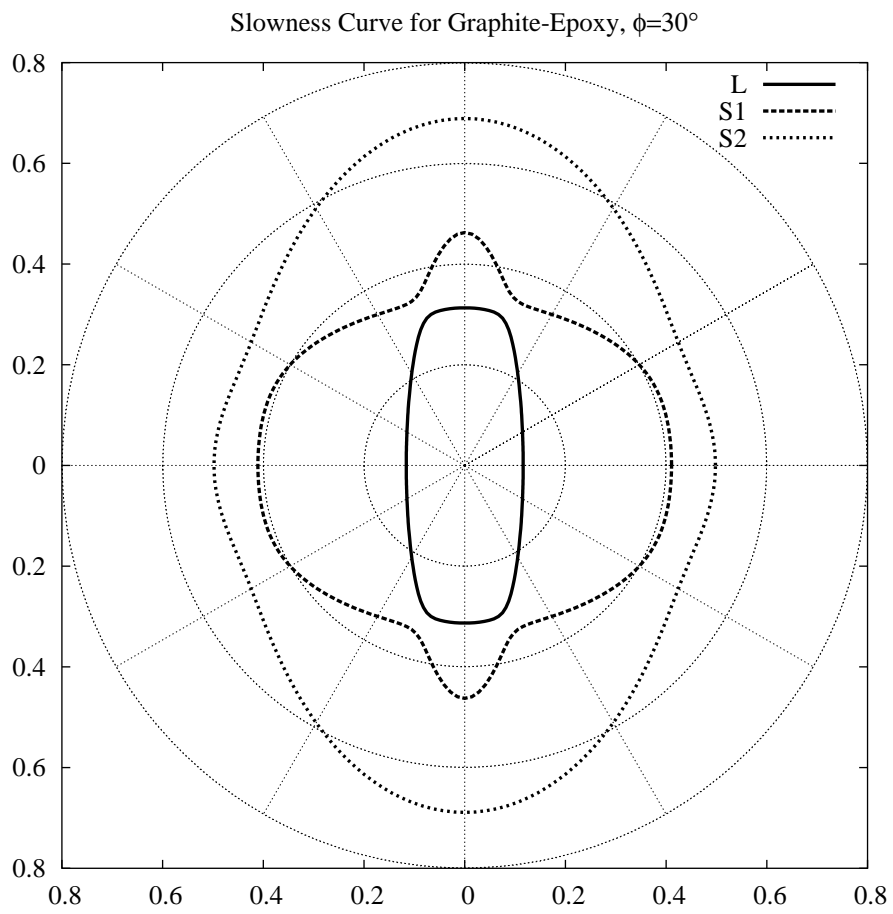


Figure 17: Skew Curve for Graphite Epoxy, $\phi = 30$

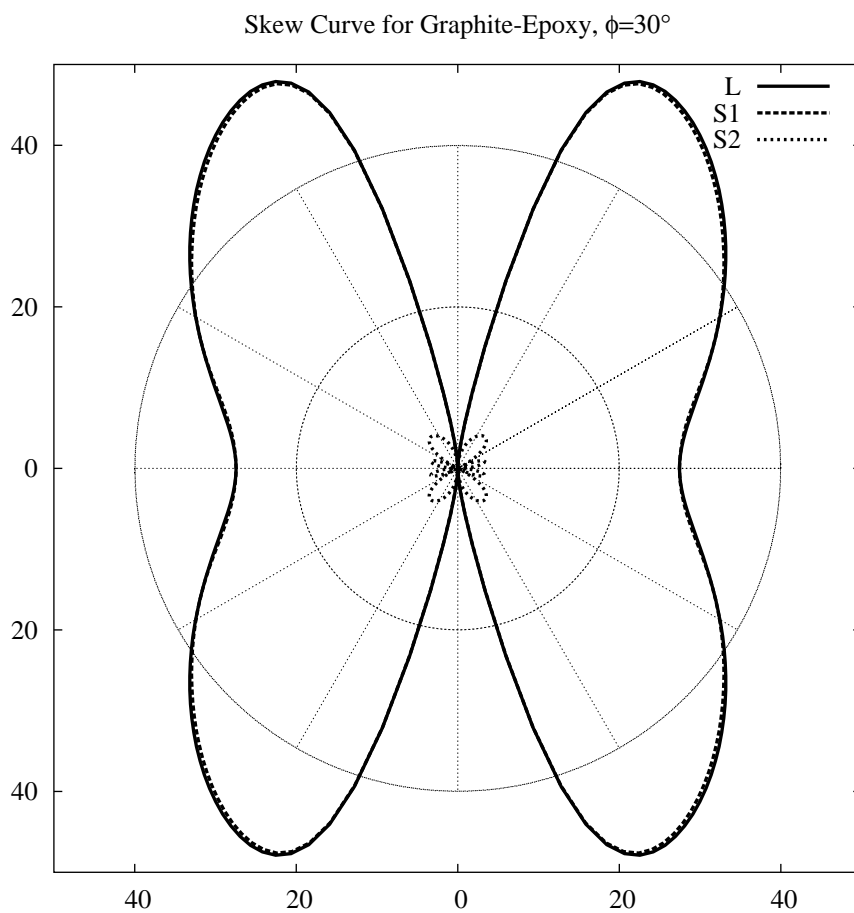


Figure 18: Slowness Curve for Quartz, $\phi = 0$, ($X - Z$ Plane)

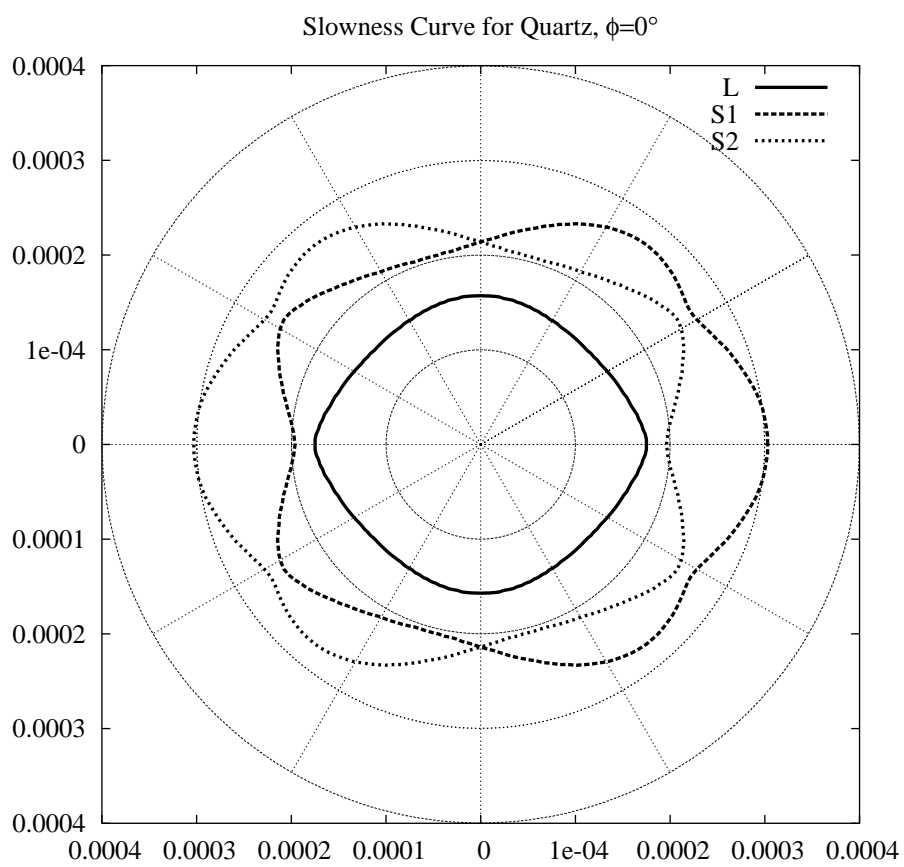


Figure 19: Skew Curve for Quartz, $\phi = 0$, ($X - Z$ Plane)

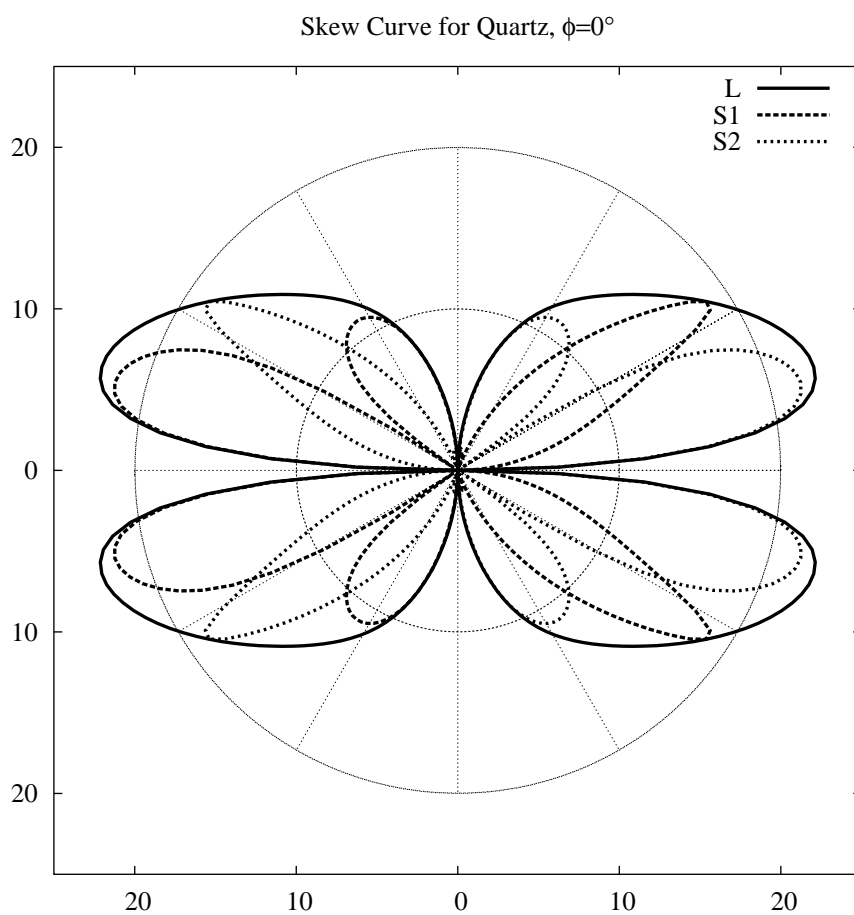


Figure 20: Slowness Curve for Quartz, $\phi = 90^\circ$, ($Y - Z$ Plane)

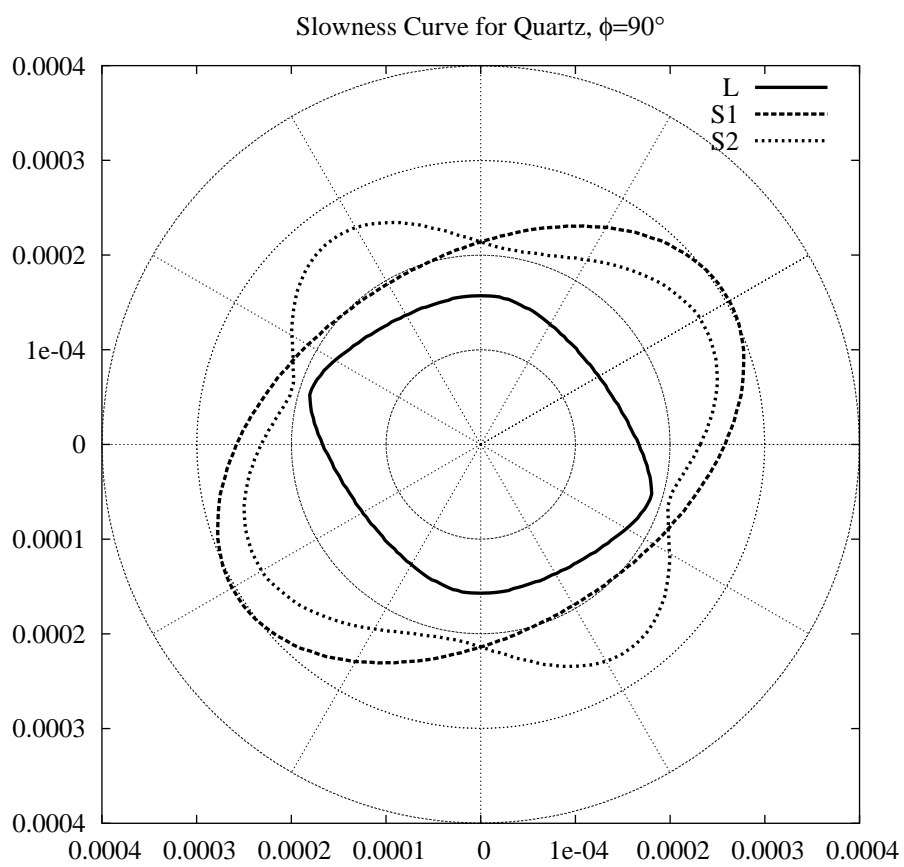


Figure 21: Skew Curve for Quartz, $\phi = 90^\circ$, ($Y - Z$ Plane)

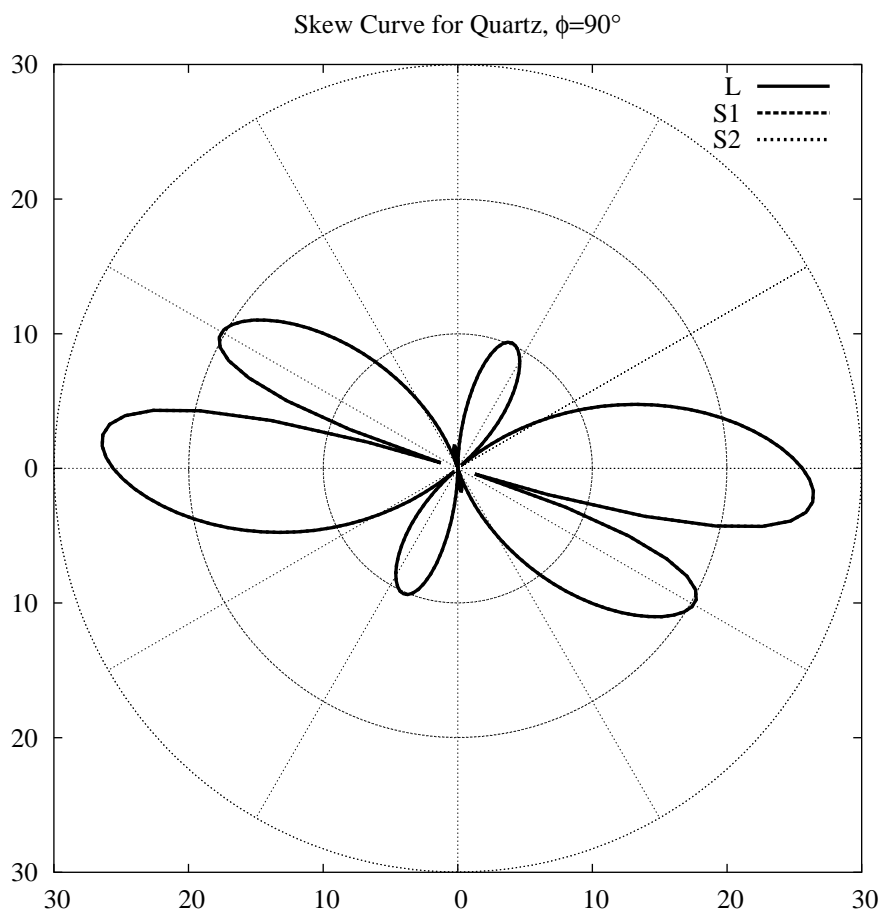


Figure 22: Slowness Curve for Quartz, $\phi = 90^\circ$, ($X - Y$ Plane)

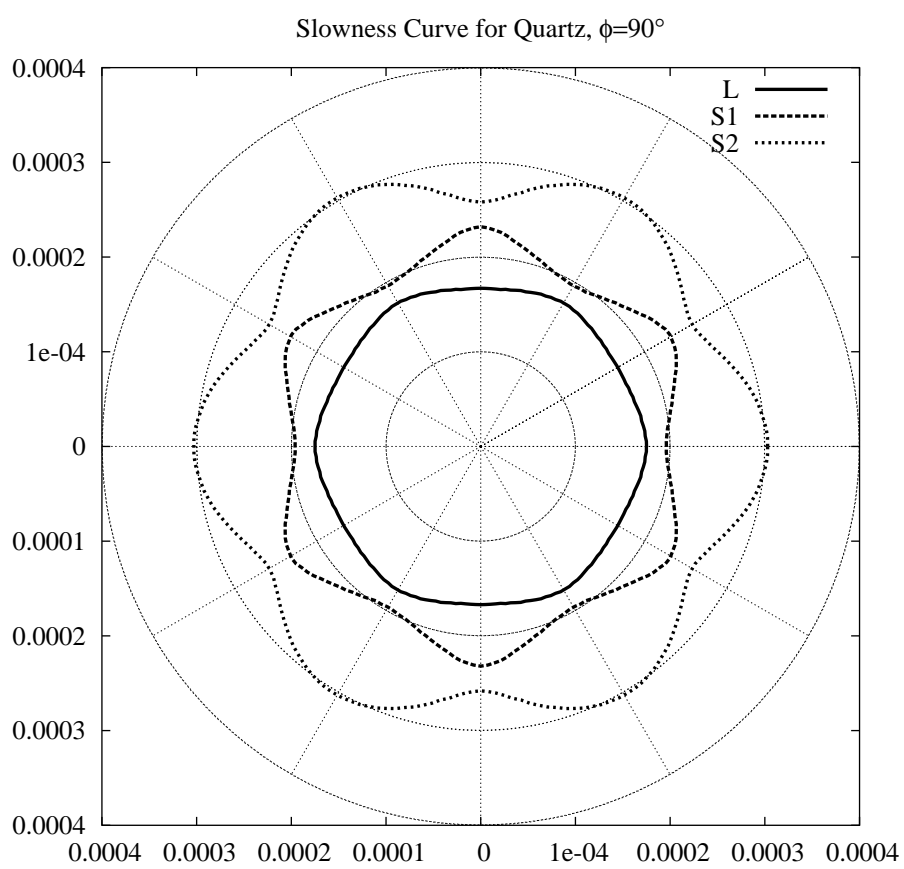


Figure 23: Skew Curve for Quartz, $\phi = 90^\circ$, ($X - Y$ Plane)

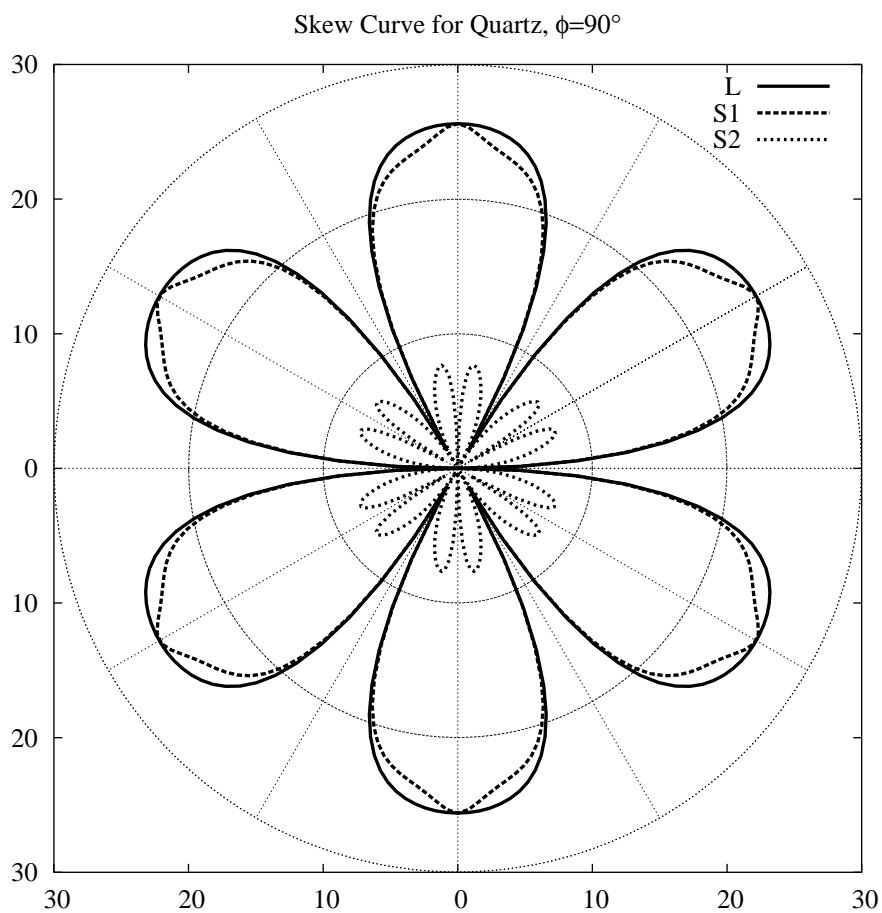


Figure 24: Slowness Curve for CdS, $\phi = 0$, ($X - Y$ Plane)

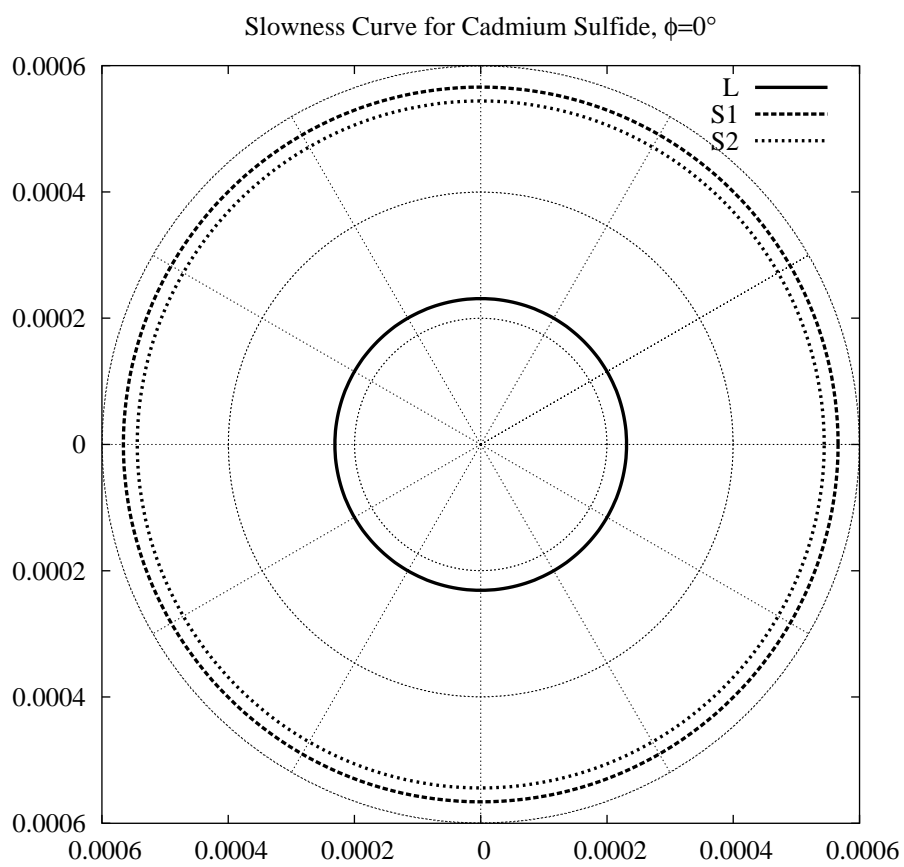


Figure 25: Skew Curve for CdS, $\phi = 0$, ($X - Y$ Plane)

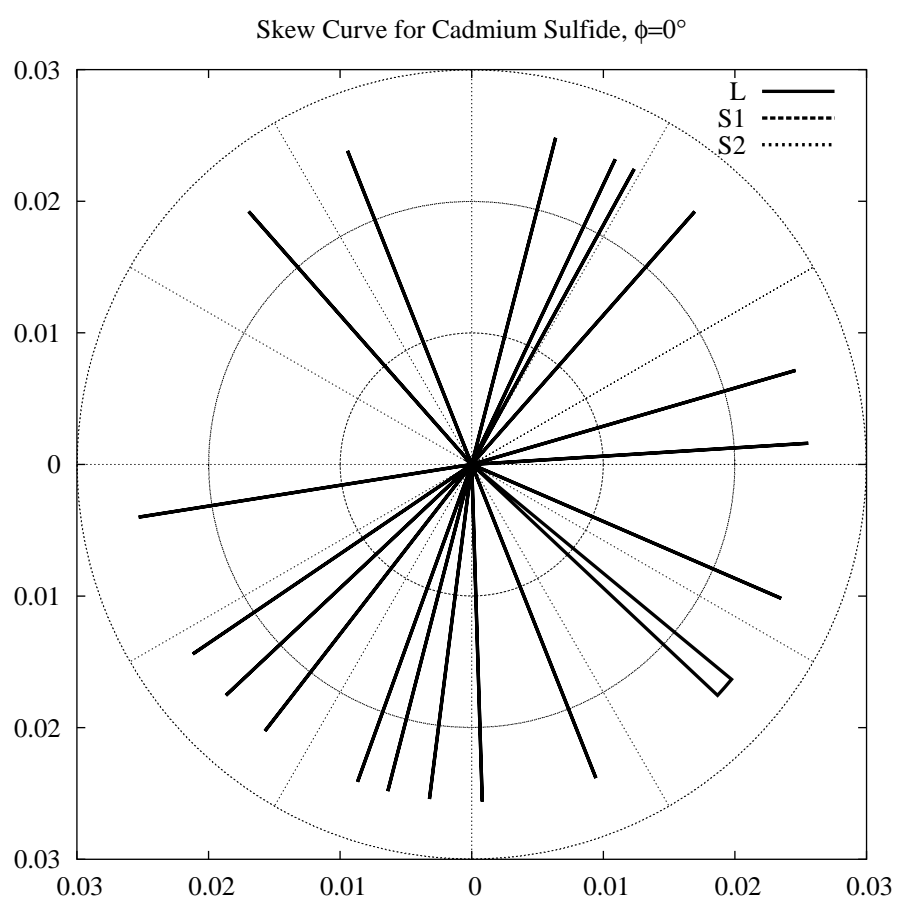


Figure 26: Slowness Curve for CdS, $\phi = 90^\circ$, ($X - Z$ Plane)

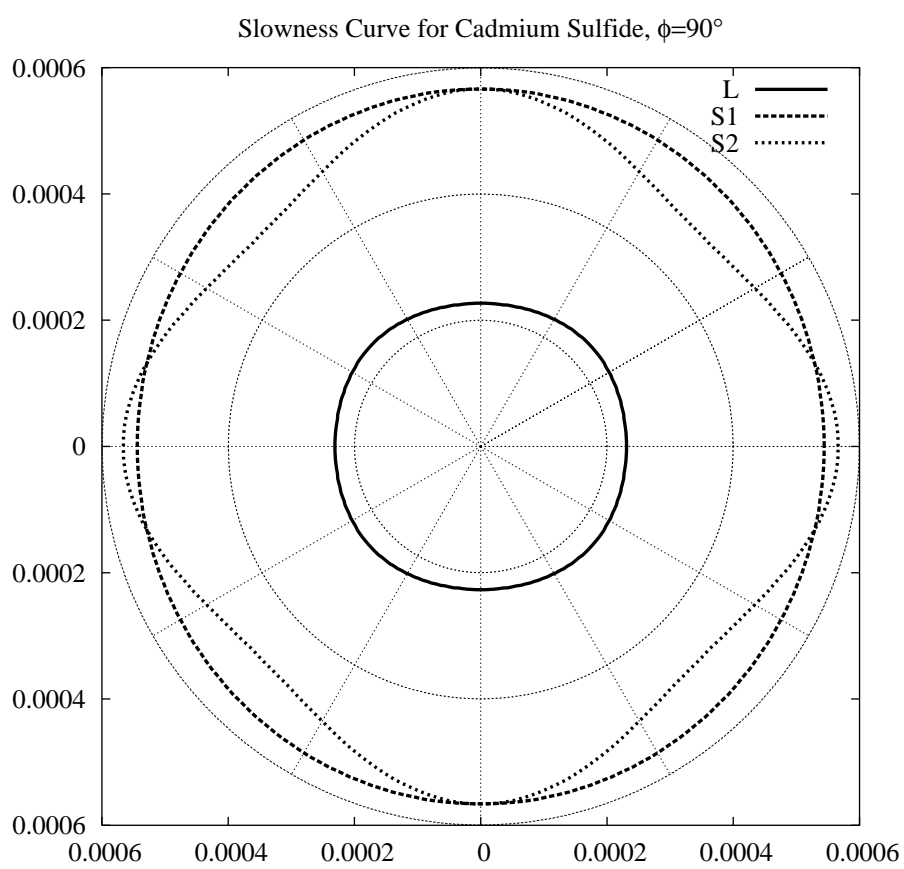
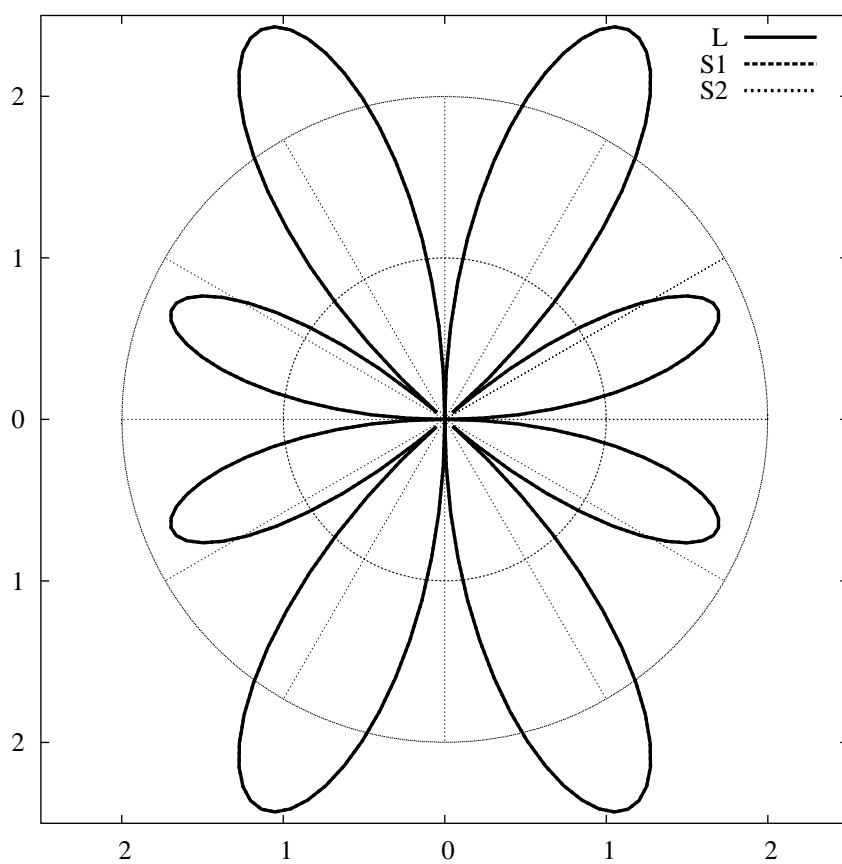


Figure 27: Skew Curve for CdS, $\phi = 90$, ($X - Z$ Plane)

Skew Curve for Cadmium Sulfide, $\phi=90^\circ$



References

- [1] B. A. Auld. *Acoustic Fields and Waves in Solids*, volume 1. John Wiley and Sons, New York, 1973.
- [2] F. I. Fedorov. *Theory of Elastic Waves in Crystals*. Plenum Press, New York, 1968.
- [3] C. Hammond. *The Basics of Crystallography and Diffraction*. Oxford University Press, Oxford, 1997.
- [4] M. A. Jaswon and M. A. Rose. *Crystal Symmetry: Theory of Colour Crystallography*. Ellis Horwood Limited, Chichester, 1983.
- [5] S. G. Lekhnitskii. *Theory of Elasticity of an Anisotropic Elastic Body*. Holden-Day, San Francisco, 1963.
- [6] A. H. Nayfeh. *Wave Propagation in Layered Anisotropic Media with Applications to Composites*. Elsevier, Amsterdam, 1995.
- [7] W. A. Wooster. *Tensors and Group Theory for the Physical Properties of Crystals*. Clarendon Press, Oxford, 1973.